J. Am. Chem. Soc. **1994,** *116,* 111-122 111

A Highly Adaptive and Strongly Binding Hemicarcerand[1,2]

Timothy A. Robbins, Carolyn B. Knobler, Donald R. Bellew, and Donald J. Cram*

Contribution from the Department of Chemistry and Biochemistry of the University of California at Los Angeles, Los Angeles, California 90024

Received August 16, 1993[⊗]

Abstract: Two new hemicarcerands (**1** and **2**) are reported, the former of which was induced to form 30 capsular complexes stable enough at 25 °C in $CDCl_3$ to be isolated and characterized. The compounds are globe-shaped and composed by attaching two tetraaryl bowls to one another at their rims through four $O(CH_2)_4O$ groups. To impart desired solubility properties to the final host, four $C_6H_5CH_2CH_2$ groups are attached to each bowl at their bases in **1**, and four $CH_3(CH_2)_4$ groups to each in **2**. The shell closure, $2\ Ar(OH)_4 + 4\ TsO(CH_2)_4OTs \rightarrow Ar[O(CH_2)_4O]_4Ar$, conducted in $(CH_3)_2NCOCH_3$–Cs_2CO_3 at 70 °C, gave **1**·$(CH_3)_2NCOCH_3$ (30–40%), and the same type of reaction in $(CH_3)_2SO$–Cs_2CO_3 gave **2**·$(CH_3)_2SO$ (15–20%), a molecule of solvent being incarcerated in each case. Empty **1** was obtained by heating **1**·$(CH_3)_2NCOCH_3$ in $(C_6H_5)_2O$ (molecules too large to be incarcerated) at 195 °C for 5 days (94%). Neat CH_2Cl_2 went in and out of the interior of **1** fast enough at 25 °C to be useful as solvent in chromatography of **1** and its complexes. By heating empty **1** at 70–170 °C for several hours up to 6 days in solutions of potential guests as solvent, or with 100 equiv of guest in $(C_6H_5)_2O$ as solvent, 30 hemicarceplexes were formed, isolated, purified, and characterized. In the crystal structure of **1**·$6H_2O$·4*o*-$(CH_3)_2C_6H_4$, the northern and southern hemispheres were twisted relative to one another around their polar axis by ~13°. The crystal structures of **1**·*p*-$I_2C_6H_4$·$2C_6H_5NO_2$, **1**·*p*-$(CH_3)_2C_6H_4$·$2NO_2C_6H_5$, **1**·$O_2NC_6H_5$·$2C_6H_5NO_2$, **1**·*o*-BrC_6H_4OH·$2C_6H_5NO_2$, and **1**·$(CH_3)_2NCOCH_3$·$2C_6H_5NO_2$ were untwisted and belonged to the same space group. The lengths along the polar axes decreased in the order listed through conformational changes in the $O(CH_2)_4O$ bridges. The E_a for decomplexation of **1**·$(CH_3)_2NCOCH_3$ in $C_6D_5NO_2$ at 140–170 °C (four temperatures) was 23.5 kcal mol^{-1}. The rotations relative to their shells of large incarcerated guests, such as 2,4-$Cl_2C_6H_3CH_3$, 3,4-$Cl_2C_6H_3CH_3$, and 4-$CH_3C_6H_4OCH_3$, were slow enough on the ^1H NMR time scale at 25 °C to produce different chemical shifts for the same host protons located in the northern and southern hemispheres of the complex. The smallest guest incorporated in **1** was Xe, but **1**·Xe as a solid gave up its guest over days at ambient temperature.

A prior paper in this series reported the dissection of the activation energies for dissociation of hemicarceplexes of **3** binding small guests, $(CH_3)_2NCOCH_3$, $CH_3CH_2COCH_3$, $CH_3CO_2CH_2CH_3$, and $C_6H_5CH_3$, into intrinsic and constrictive binding free energy terms.[3] A second paper[4] surveyed the binding properties of **4**, whose inner phase is much larger, and whose four portals connecting the inner and outer phases were 30-membered rings, in contrast to the 26-membered rings of **1–3**. The largest guests introduced into **3** at high temperatures, such as *p*-$(CH_3)_2C_6H_4$ or $CH_3CH_2C_6H_5$, were too small to be retained at low temperatures by **4**,[3] which formed stable complexes with molecules as large as 1,3,5-$[(CH_3)_2CH]_3C_6H_3$, [3.3]paracyclophane, and 4-ethyl[2.2]paracyclophane.[4]

The current paper reports the synthesis of **1** and **2**, the crystal structures of **1**·$6H_2O$·4*o*-$(CH_3)_2C_6H_4$, **1**·*p*-$I_2C_6H_4$·$2C_6H_5NO_2$, **1**·*p*-$(CH_3)_2C_6H_4$·$2NO_2C_6H_5$, **1**·$O_2NC_6H_5$·$2C_6H_5NO_2$, **1**·*o*-BrC_6H_4OH·$2NO_2C_6H_5$, and **1**·$(CH_3)_2NCOCH_3$·$2NO_2C_6H_5$, and a survey of the binding properties of **1** toward many potential guests that range in size from Xe to $(C_6H_5)_2O$ (Ph_2O). Although the number of atoms composing the portals of both **1** and **3** is 26, the presence of the *o*-xylyl units in **3** constrains the macroring portals to conformations that accommodate the enforced coplanarity of the four spanning carbon atoms, whereas no such constraints apply to the four spanning carbon atoms of the $(CH_2)_4$ units of **1** or **2**. Not only should the portals of **1** or **2** be more adaptive to the shapes of entering guests but the shells of the resulting carceplexes are more amenable to forming close contacts and minimizing their unoccupied internal volumes than are those of **3**. Therefore, it seemed likely that **1** and **2** should bind not only a wider range of guests with respect to size and shape than **3** but also to complex their guests more strongly. Both **1** and **2** were synthesized because past experience has shown that $C_6H_5CH_2CH_2$ groups appended to carcerands and hemicarcerands tend to produce better crystals for structure determination, whereas those with $CH_3CH_2CH_2CH_2CH_2$ appended groups (feet) tend to be soluble in a greater range of solvents.[4,5] Experimentally, **1** with $C_6H_5CH_2CH_2$ feet turned out to give good crystals and to possess desired solubility properties, so it was the only one whose complexation properties were examined.

Results

Syntheses. Tetrols **5**[6] and **6**[4] were available from earlier investigations. Treatment of **5** with $Br(CH_2)_4Br$–NaI–Cs_2CO_3–$(CH_3)_2NCOCH_3$ at 80 °C without high dilution gave **1**·$(CH_3)_2NCOCH_3$ in 15% yield. Under high dilution conditions, the shell-closing reaction of **5** with $TsO(CH_2)_4OTs$–Cs_2CO_3–$(CH_3)_2NCOCH_3$ at 70 °C went in 30–40% yields, whereas when $(CH_3)_2SO$ was employed as solvent, **1**·$(CH_3)_2SO$ was produced in 20% yield. When **2** was similarly shell closed, a 15–20% yield of **2**·$(CH_3)_2SO$ was obtained.

Initial studies of decomplexing **1**·$(CH_3)_2NCOCH_3$ were carried out by heating the hemicarceplex in $2NO_2$–1,3-$(CH_3)_2C_6H_3$. This solvent was chosen because Corey–Pauling–Koltun (CPK) model examination indicated it to be too large to pass through the 26-membered-ring portals of **1**. In practice, a 2-day heating of **1**·$(CH_3)_2NCOCH_3$ at 185 °C in this solvent gave mainly **1** mixed

---

[⊗] Abstract published in *Advance ACS Abstracts,* December 1, 1993.

(1) Host–guest complexation #67.

(2) We warmly thank the U.S. Public Health Services for supporting Grant GM-12640, and the National Science Foundation for supporting Grant NSF CHE 8802800.

(3) Cram, D. J.; Blanda, M. T.; Paek, K.; Knobler, C. B. *J. Am. Chem. Soc.* **1992**, *114*, 7765–7773.

(4) Cram, D. J.; Jaeger, R.; Deshayes, K. *J. Am. Chem. Soc.*, in press.

(5) Cram, D. J. *Nature* **1992**, *356*, 29–36.

(6) Sherman, J. C.; Knobler, C. B.; Cram. D. J. *J. Am. Chem. Soc.* **1991**, *113*, 8909-8916.

0002-7863/94/1516-0111$04.50/0

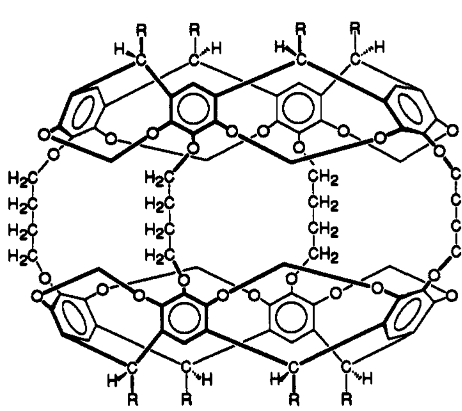

1, R = $C_6H_5CH_2CH_2$; **2**, R = $CH_3CH_2CH_2CH_2CH_2$

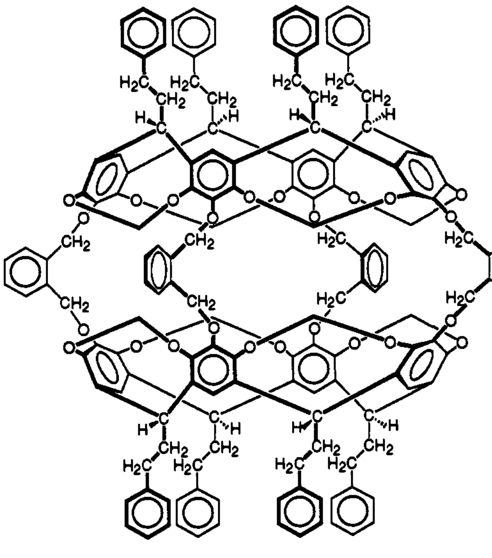

3

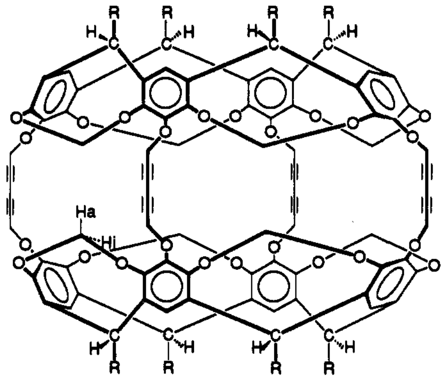

4, R = $CH_3CH_2CH_2CH_2CH_2$

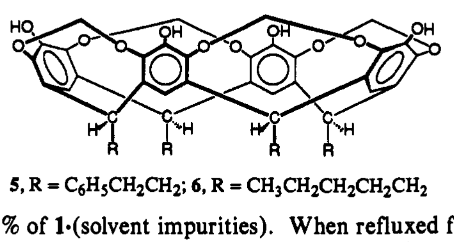

5, R = $C_6H_5CH_2CH_2$; **6**, R = $CH_3CH_2CH_2CH_2CH_2$

with 3–5% of **1**·(solvent impurities). When refluxed for 2 days in 1,3,5-$[(CH_3)_3C]_3C_6H_3$, **1**·$(CH_3)_2NCOCH_3$ failed to give incarcerated *hydrocarbon*, as expected from molecular model examination. A model of $(C_6H_5)_2O$ (Ph_2O) also proved impossible to be placed in the interior of a model of **1**. This ether is a powerful solvent that possesses a bp of 260 °C and a liquid range of about 230 °C and is easy to purify. When **1**·$(CH_3)_2NCOCH_3$ dissolved in Ph_2O was heated at 195 °C for 5 days, or at reflux for 2 days, respective yields of 94% and 85–90% of empty **1** were realized. When CH_2Cl_2–hexane or CH_2Cl_2–EtOAc was used to chromatograph empty **1**, hexane and EtOAc, respectively, became incarcerated in **1**. Neat CH_2Cl_2 was found to be the best solvent for chromatography. Neat $CHCl_3$ entered **1** as well, but did not depart the interior fast enough to be useful in chromatography. Even washing solid **1** with pentane resulted in incarceration of the pentane. By the time "empty" **1** had been flown from Los Angeles to Arizona, where it underwent elemental analysis, it had incarcerated one or two molecules of water. By the time its crystal structure was determined 6 months later, six molecules of H_2O had adventitiously entered the inner phase of each molecule of host.

Incarceration Experiments. Incarceration experiments were carried out either by heating empty **1** in the solvent (degassed) whose molecules were to be imprisoned or in solutions of 100 equiv of potential solid guest to 1 equiv of empty **1** in degassed Ph_2O. Temperatures of 70–170 °C and times of several days were employed for forming 1:1 complexes. The final solutions were cooled, and the complexes were precipitated by addition of methanol and dried. Table I reports those hemicarcerands that were isolated, the times and temperatures of host–guest contacts, elemental analyses for the 24 complexes that appeared to be homogeneous and 1:1 by their ^1H NMR spectra, low-resolution FABMS peaks for **1**·G and **1** (m/e and % of $M^+ + 1$), and the numbers of atoms other than hydrogen in the guest.

All of the complexes listed in Table I were characterized by their ^1H NMR spectra (500 MHz, $CDCl_3$, 25 °C). Certain host- and guest-proton chemical shifts changed upon complexation. The host signals most sensitive to guests are those due to H_i and H_a, which are respectively the inwardly- and axially-oriented protons of the eight intrahemispheric bridges. The host signals next most sensitive to guest presence were the eight ArH protons labeled H_p which are aimed at the north and south poles of the globes. The methine protons labeled H_m of the $Ar_2RC\mathit{H}$ protons are aimed away from the globe and are the most distant and least sensitive to guest character. Table II lists H_i, H_a, H_p, and H_m chemical shifts relative to $(CH_3)_4Si$ (δ), as well as $\Delta\delta$ values, which are the chemical shift values of **1** minus those for **1**·Guest.

The guest signals were much more sensitive than the host signals to incarceration. Table III lists the 500-MHz δ values and their multiplicities in $CDCl_3$ at 25 °C of simple dissolved guests, those of their complexes, and the chemical shifts of the free guests minus those for the complexed guests ($\Delta\delta$ values).

Decomplexation Activation Free Energy of 1·$(CH_3)_2NCOCH_3$. First-order rates for decomplexing **1**·$(CH_3)_2NCOCH_3$ in degassed $C_6D_5NO_2$ were followed by the large changes in the ^1H NMR spectra of incarcerated and free guest to give the following respective rate constant and $t_{1/2}$ values: 140 °C, $5.17 \times 10^{-5}\ s^{-1}$, $t_{1/2}$ 223 min; 150 °C, $8.23 \times 10^{-5}\ s^{-1}$, $t_{1/2}$ 140 min; 160 °C, $1.88 \times 10^{-4}\ s^{-1}$, $t_{1/2}$ 61 min; 170 °C, $3.77 \times 10^{-4}\ s^{-1}$, $t_{1/2}$ 30 min. These provide an E_a value of $23.5 \pm 1.5\ kcal\ mol^{-1}$ for the decomplexation in this solvent. An earlier study of **3**·$(CH_3)_2NCOCH_3$ demonstrated that rate constants for decomplexation varied by more than 2 powers of 10 with solvent changes[3] and that $C_6D_5NO_2$ provided the fastest rate for decomplexation.[7]

Crystal Structures. Crystal structures of **1**·$6H_2O$·4*o*-xylene (R, 0.15), **1**·*p*-$I_2C_6H_4$·$2C_6H_5NO_2$ (R, 0.11), **1**·*p*-$(CH_3)_2C_6H_4$·$2C_6H_5NO_2$ (R, 0.22), **1**·$O_2NC_6H_5$·$2C_6H_5NO_2$ (R, 0.15), **1**·*o*-BrC_6H_4OH·$2C_6H_5NO_2$ (R, 0.21), and **1**·$(CH_3)_2NCOCH_3$·$2C_6H_5NO_2$ (R, 0.22) were determined. Chart Iprovides a full drawing of **1**·Guest and side views of stereodrawings of each of the crystal structures. The partially disordered *o*-xylene is omitted from the view of **1**·$6H_2O$, but the two solvating $C_6H_5NO_2$ molecules are included in the views of the other five crystal structures. Also included are part views along the polar axis of the hemicarceplexes which include the guest but omit all of the host except the $[O(CH_2)_4O]_4$ interhemispheric bridges. In these

---

[7] Blanda, M. T.; Cram, D. J. Unpublished results.

Table I. Conditions Under Which Guests Formed One-to-One Hemicarceplexes with **1**, Elemental Analyses, and FAB Mass Spectral Signals of Complexes

				MS (M$^+$) obs (%)[a]		elemental analyses (%)						
						calculated			found			
guest	solvent	time (days)	T (°C)	e/m complex	e/m host	C	H	hetero	C	H	hetero	no. of non-H guest atoms
$2H_2O$	Ph_2O	5	195		2251 (100)	75.64[b]	6.17[b]		75.42	6.00		2
$1H_2O$	Ph_2O	5	195			76.18[c]	6.12[c]		76.18	6.12		1
Xe[d]	CH_2Cl_2	1	25			72.61	5.75		75.27	5.81		1
CH_3CH_2I	guest	3.5	72	2467 (100)	2251 (50)	72.87	5.91	5.27 (I)	72.80	5.95	7.79 (I)	3
CH_3COCH_3	Ph_2O	3.5	57		2251 (100)	76.48	6.20		76.80	5.99		4
$(CH_3)_2SO$	guest[e]	3	70	2329 (100)		75.30	6.15	1.38 (S)	75.02	6.12	1.00 (S)	4
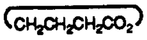 $CH_2CH_2CH_2CO_2$	guest	4	170			76.07	6.12		76.02	6.17		6
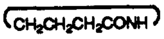 $CH_2CH_2CH_2CONH$	Ph_2O	3	100									
$CH_3CH_2O_2CCH_3$	Ph_2O	3.5	77	2339 (100)	2251 (80)	76.01	6.21		76.25	6.12		6
$(CH_3)_2NCOCH_3$	guest[f]	4	80	2338 (100)	2249 (30)	76.04	6.25	0.60 (N)	76.23	6.14	0.43 (N)	6
 $CH{=}CHCOCH_2CH_2$	guest	5	140									6
 $CH_2CH_2COCH_2CH_2$	guest	5	130	2335 (100)	2250 (40)	76.65	6.22		76.63	6.33		6
C_6H_6	guest	5	80	2329 (100)		77.37	6.15		77.14	6.04		6
$C_6H_5NH_2$	guest	5	145	2344 (100)	2252 (35)	76.87	6.15	0.60 (N)	77.23	6.01	0.63 (N)	7
C_6H_5I	guest	3	170			73.39	5.78		74.59	5.90		7
1,4-$Br_2C_6H_4$[b]	guest	3	155			72.45	5.65	6.43 (Br)	72.52	5.59	6.39 (Br)	8
1,4-$I_2C_6H_4$	Ph_2O	4.5	160	2583 (100)	2251 (50)	69.82	5.47	9.84 (I)	70.21	5.45	9.80 (I)	8
1,4-$(HO)_2C_6H_4$	Ph_2O	4.5	140	2360 (100)	2251 (35)	76.32	6.06		95.93	6.12		8
1,2-$(HO)_2C_6H_4$	Ph_2O	4.5	140	2360 (100)	2252 (22)	76.32	6.06		76.11	5.97		8
1,4-$(CH_3)_2C_6H_4$	guest	4	138	2357 (100)	2251 (55)	77.46	6.24		77.53	6.32		8
1,3-$(CH_3)_2C_6H_4$[g]	guest	4	139	2356 (85)	2251 (100)	74.34	5.86	3.30 (Br)	74.70	5.94	3.38 (Br)	8
2-BrC_6H_4OH	guest	3.5	140	2424 (100)	2251 (40)	76.82	6.10		76.84	5.91		8
4-$FC_6H_4CH_3$[b]	guest	4	116			75.90	5.99	0.59 (N)	76.29	5.77	0.42 (N)	9
$C_6H_5NO_2$	guest	4.5	170	2374 (100)	2251 (30)							9
4-$CH_3C_6H_4OCH_3$	guest	3.5	170			76.37	6.11		76.56	6.04		9
2,5-$(HO)_2C_6H_3CH_3$	Ph_2O	4.5	140	2375 (100)	2251 (18)	76.37	6.11		76.19	5.93		9
3,4-$(HO)_2C_6H_3CH_3$	Ph_2O	4.5	140	2375 (100)	2251 (30)	75.20	5.93	2.93 (Cl)	75.03	5.62	2.61 (Cl)	9
2,4-$Cl_2C_6H_3CH_3$	guest	3.5	170	2413 (60)	2252 (100)	75.20	5.93	2.93 (Cl)	76.48	5.83	2.48 (Cl)	9
3,4-$Cl_2C_6H_3CH_3$	guest	3.5	170	2412 (100)	2251 (95)	76.43	6.16		76.54	6.04		10
1,4-$(CH_3O)_2C_6H_4$	Ph_2O	4.5	140	2390 (100)	2251 (10)	73.93	5.62		73.98	5.55		12
C_6F_6	guest	2	80									

[a] FABMS, 3-$NO_2C_6H_4CH_2OH$ matrix. [b] **1**·$2H_2O$. [c] **1**·H_2O (samples of footnotes *b* and *c* were independently prepared and dried). [d] Xe was lost slowly at 25 °C from the solid state of its complex. [e] Made by shell closure in $(CH_3)_2SO$. [f] Made by shell closure in $(CH_3)_2NCOCH_3$. [g] 2:1 mixture of meta:para isomers.

part structures, the sets of four oxygens of the southern and northern hemispheres each form a near square, as shown by heavy lines connecting each set of four oxygens. The planes of these squares in **1**·$6H_2O$ are nearly parallel and in the other five crystal structures are parallel to one another. The rotations of these squares with respect to one another provide an indication of how much the northern and southern hemispheres are twisted around the north–south polar axes with respect to one another.

Discussion

Conformations Available to 1. All six crystal structures of complexes of **1** containing six H_2O, *p*-$I_2C_6H_4$, *p*-$(CH_3)_2C_6H_4$, $O_2NC_6H_5$, *o*-BrC_6H_4OH, and $(CH_3)_2NCOCH_3$ as guests in their top views (Chart I) indicate that the four $(CH_2)_4$ interhemispheric bridging groups lie outside the volumes defined by connecting the eight ArO oxygens of the host with imaginary straight lines. To provide this type of geometry, the unshared electron pairs of all eight oxygens must face inward toward the cavity, and their bonds to the methylene bridges must diverge from the cavity. This arrangement provides an *out–in–out* orientation of unshared electron pairs for the three oxygens attached to adjacent carbons on each of the eight benzene rings of the host and provides for the greatest compensation of dipoles and lowest energy. An alternate *in–out–in* arrangement of these oxygens is impossible to construct using CPK models since the methine and one hydrogen of the OCH_2O bridge cannot occupy the same space at the same time.

In CPK models of **1**, when the $(CH_2)_4$ interhemispheric bridges of **1** are all distributed outside of their attached oxygens, as in views **8**–**18** of the six crystal structures, the 26-membered-ring portal is generally widest in the horizontal dimension, as in **9** and **11**, but is shortest in the vertical dimension. We label this conformation $(BO)_4$, meaning *four bridges out.* At the other general extreme, the unshared electron pairs of the eight oxygens of the $[O(CH_2)_4O]_4$ bridges face outward, forcing the four-carbon $(CH_2)_4$ chains inward. In this conformation, the portal and cavity become longer in the vertical dimension, but shorter in the horizontal dimension. We label this conformation $(BI)_4$, meaning *four bridges in.* Many other combinations and permutations are possible, each of which modifies the shape of the portals somewhat, but they all have an overall slot-shaped character.

A second important structural feature of models of **1** is that, in the $(BO)_4$ conformation, the northern and southern polar caps can twist with respect to one another around their common polar axis, as is visible in **8**. This twist when taken to its extreme of about 15° completely closes the portals, brings the polar caps into contact with one another at their rims, severely reduces the cavity size, and increases the numbers of atom-to-atom contacts (rim-to-rim plus rim-to-bridge) by 56, 32 of which are of the H···O variety, which should be particularly stabilizing. The number 56 exceeds the number 31 contacts added by fully twisting host **3**,[3] which contains $(1,2\text{-}OCH_2C_6H_4CH_2O)_4$ spanning groups. The 25 additional contacts in **1** account for the higher activation energies and temperatures required for complexing and decomplexing **1** involving small guests compared to **3**.[3]

The maximum twist for the $(BO)_4$ conformation of **1** can just be reached when the model contains a spherical guest of a diameter about 4.5 Å, close to the diameter of Xe at 4.4 Å (measured in

Table II. Chemical Shifts of Host's Guest-Sensitive Protons and the Differences between the Chemical Shifts of Free and Complexed Hosts in Their ^{1}H NMR Spectra in $CDCl_3$ at 25 °C

	H_i of OCH_2O		H_a of OCH_2O		H_p of ArH		H_m of Ar_2RCH	
guest	δ	$\Delta\delta$	δ	$\Delta\delta$	δ	$\Delta\delta$	δ	$\Delta\delta$
none	4.30		5.80		6.83		4.81	
Xe	4.19	0.11	5.81	-0.01			4.82	-0.01
CH_3CH_2I	4.20	0.10	5.86	-0.06	6.82	0.01	4.80	0.01
CH_3COCH_3	4.09	0.21	5.87	-0.07	6.85	-0.02	4.83	-0.02
$(CH_3)_2SO$	4.18	0.12	5.85	-0.05	6.85	-0.02	4.85	-0.04
$CH_3CH_2O_2CCH_3$	4.21	0.09	5.83	-0.03	6.82	0.01	4.83	-0.02
$CH_2CH_2COCH_2CH_2$	4.15	0.15	5.79	0.01	6.86	-0.03	4.84	-0.03
$(CH_3)_2NCOCH_3$	4.29	0.01	5.81	-0.01	6.84	-0.01	4.85	-0.04
$CH_2CH_2CH_2CO_2$	4.14	0.16	5.83	-0.03	6.86	-0.03	4.81	0.00
$CH_2CH_2CH_2CONH$	4.21	0.09	5.82	-0.02	6.87	-0.04	4.81	0.00
$CH{=}CHCOCH_2CH_2$	4.13	0.17	5.79	0.01	6.88	-0.05	4.83	-0.02
$CH_2CH_2COCH_2CH_2$	4.15	0.15	5.79	0.01	6.86	-0.03	4.84	-0.03
C_6H_6	4.05	0.25	5.70	0.10	6.97	-0.14	4.85	-0.04
C_6F_6	4.31	-0.01	5.78	0.02	6.86	-0.03	4.86	-0.05
$C_6H_5NH_2$	4.16	0.14	5.69	0.11	6.92	-0.09	4.85	-0.04
C_6H_5I	4.42, 4.11	-0.12, 0.19	5.66	0.14	6.83	0.00	4.83	-0.02
1,4-$Br_2C_6H_4$	4.12	0.18	5.72	0.08	6.83	0.00	4.85	-0.04
1,4-$I_2C_6H_4$	4.25	0.05	5.69	0.11	6.76	0.07	4.88	-0.07
1,4-$(HO)_2C_6H_4$	4.39	-0.09	5.80	0.00	6.80	0.03	4.81	0.00
1,2-$(HO)_2C_6H_4$	4.23	0.07	5.69	0.11	6.92	-0.09	4.84	-0.03
1,4-$(CH_3)_2C_6H_4$	4.14	0.16	5.68	0.12	6.88	-0.05	4.87	-0.06
1,3-$(CH_3)_2C_6H_4$	4.24	0.06	5.65	0.15	6.92	-0.09	4.85	-0.04
2-BrC_6H_4OH	4.23	0.07	5.65	0.15	6.86	-0.03	4.85	-0.04
4-$FC_6H_4CH_3$	4.10	0.20	5.71	0.09	6.84	-0.01	4.83	-0.02
$C_6H_5NO_2$	4.06	0.24	5.62	0.18	6.84	0.01	4.84	-0.03
4-$CH_3C_6H_4OCH_3$	4.17, 4.25	0.13, 0.05	5.68, 5.70	0.12, 0.10	6.84, 6.89	-0.01, -0.06	4.87	-0.06
2,5-$(HO)_2C_6H_3CH_3$	4.30	0.00	5.66	0.14	6.93	-0.10	4.84	-0.02
3,4-$(HO)_2C_6H_3CH_3$	4.22	0.08	5.68	0.12	6.90	-0.07	4.85	-0.04
2,4-$Cl_2C_6H_3CH_3$	4.10, 4.33	0.20, -0.03	5.68, 5.70	0.12, 0.10	6.86, 6.92	-0.03, -0.09	4.76	0.05
3,4-$Cl_2C_6H_3CH_3$	4.06, 4.37	0.24, -0.07	5.66, 5.70	0.14, 0.10	6.87, 6.88	-0.04, -0.05	4.86	-0.05
1,4-$(CH_3)_2C_6H_4$	4.28	0.02	5.70	0.10	6.83	0.00	4.90	-0.09

a clathrate crystal).[8] A molecular model of CH_2Cl_2 easily enters and departs **1** with its portals open, and rattles inside the fully twisted model of **1**. A model of $CHCl_3$ can just be pushed through the open portal of **1** and is large enough to slightly inhibit the maximum twisting of **1**. Although models of CCl_4 and $CHCl_2CHCl_2$ cannot be pushed through the open portal of **1**, they easily fit inside if bonds are broken and made to get them in. These last two compounds are too large to allow much twisting of the hemispheres in models of **1**, as is true for *p*-$I_2C_6H_4$, *p*-$(CH_3)_2C_6H_4$, $O_2NC_6H_5$, *o*-BrC_6H_4OH, and $(CH_3)_2NCOCH_3$.

Binding of Guests by 1. Aside from Xe, the 29 guest molecules that were incarcerated successfully in empty **1** fall into classes A–F with regard to their shapes, which are formulated in Chart II. Class A contains acyclic compounds of three to six non-hydrogen atoms containing zero to two branches. Models of complexes **1**·A are easily assembled without breaking and making bonds, and except for **1**·$(CH_3)_2NCOCH_3$, the guests are small enough for all the northern and southern hemispheres to twist sufficiently to bring the rims of the two hemispheres into contact with one another, which could contribute substantially to the kinetic stability of the complexes. However, the ^{1}H NMR spectra of those hemicarceplexes containing non-like-ended guests, such as CH_3CH_2I, $(CH_3)_2NCOCH_3$, and $CH_3CH_2O_2CCH_3$, show the presence of only *one kind* of H_i and H_a signals, which means that at 25 °C the guests can all rotate rapidly on the ^{1}H NMR time scale relative to their host (see Table II). Model examination indicates that equilibration between different orientations of guest with respect to host can occur only when the host is untwisted. An alternate way to twisting that allows the host to be complementary to varying guest size is shrinking the effective length of the $(CH_2)_4$ bridges by conformational adjustments most visible in a comparison of **10** and **18**. In passing from the longest guest (*p*-$I_2C_6H_4$) to the shortest [$(CH_3)_2NCOCH_3$], the CH_2*CH_2*–*CH_2*CH_2 central bond in the bridges approaches coplanarity with a plane perpendicular to the polar axis of the hemicarceplex.

The guest's methyl groups' ^{1}H NMR spectral signals are changed by incarceration by values for $\Delta\delta$ that vary between a low of 1.33 (H_b of $(CH_3)_2NCOCH_3$, Table III) and a high of 4.23 (H_a of $CH_3COCH_2CH_3$, Table III). Of the guests of group A, these two provide the longest chain of four carbons, which pushes the methyls on the long axis of the guest the farthest into the shielding polar regions of the host.

The generally slot-shaped cross sections of cyclic class B guests in models are easier to push through the slot-shaped portals of **1** than are the more conformationally mobile guests of class A. The $\Delta\delta$ values for H_i of the host of **1**·A vary from a low of 0.01 in **1**·$(CH_3)_2NCOCH_3$ to a high of 0.21 ppm for **1**·CH_3COCH_3, with the $\Delta\delta$ values for **1**·B ranging only from 0.09 to 0.17 ppm. The CH_2 protons of the cyclic guests cannot in models penetrate as deeply into the shielding polar regions of the host as do the CH_3 protons of guests in the **1**·A group of complexes. The $\Delta\delta$ values are therefore lower for the former than for the latter, ranging from 3.29 to 1.56 ppm. All of the protons of $CH_2CH_2CH_2CONH$ provide lower $\Delta\delta$ values than those of the other cycles. Hydrogen bonding between this guest and the inward-turned unshared electron pairs of the $ArOCH_2$ oxygens tends to orient the whole cycle in the equatorial region of the cavity where the least shielding is felt.

All of the aromatic guests of classes C–F possess slot-shaped cross sections, and their atoms all tend to be coplanar except the methyl moieties of 1,4-$(CH_3O)_2C_6H_4$. In models with tightly fitting (nonoxidized) connectors, all of these guests can be introduced into **1** without breaking bonds, and for the larger guests only with difficult and synchronous conformational changes of the host. To fully twist the hemispheres of the host, the axis of C_6H_6 as guest must assume a north–south pole alignment. As the guests become more highly substituted, this alignment becomes more mandatory, and the twisting of the host's hemispheres is inhibited more, so that by the time 1,4-$(CH_3)_2C_6H_4$ or 1,4-$I_2C_6H_4$ is reached, little twisting is possible.

As expected, these aromatic guests generally affect the $\Delta\delta$ values of the H_i host protons more than do the nonaromatic guests.

---

[8] Lee, F.; Gabe, E.; Tse, T. S.; Ripmeester, J. A. *J. Am. Chem. Soc.* **1988**, *110*, 6014–6019.

Table III. Chemical Shifts of Free and Incarcerated Guests' Protons and the Differences in Their ^1H NMR Spectra in $CDCl_3$ at 25 °C

guest structure	δ of free guest (multiplicity)	δ of complexed guest (multiplicity)	Δδ
$\overset{a}{CH_3}\overset{b}{CH_2}I$	H_a, 1.84 (t)	H_a, −1.32 (t)	3.16
	H_b, 3.19 (q)	H_b, 1.35 (q)	1.84
$\overset{a}{CH_3}COCH_3$	H_a, 2.17 (s)	H_a, −0.83 (s)	3.00
$\overset{a}{CH_3}SOCH_3$	H_a, 2.46 (s)	H_a, −0.49 (s)	2.95
$\overset{a}{CH_3}CO_2\overset{b}{CH_2}\overset{c}{CH_3}$	H_a, 2.04 (s)	H_a, −2.19 (s)	4.23
	H_b, 4.11 (q)	H_b, 2.28 (q)	1.83
	H_c, 1.25 (t)	H_c, −1.97 (t)	3.22
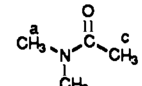	H_a, 3.02 (s)	H_a, −0.42 (s)	3.44
	H_b, 2.94 (s)	H_b, 1.61 (s)	1.33
	H_c, 2.08 (s)	H_c, −1.64 (s)	3.72
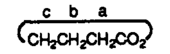 $\overset{c}{CH_2}\overset{b}{CH_2}\overset{a}{CH_2}CO_2$	H_a, 3.74 (m)	H_a, 0.50 (t)	3.24
	H_b, 2.89 (m)	H_b, 0.27 (t)	2.62
	H_c, 5.35 (t)	H_c, 1.66 (t)	3.69
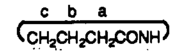 $\overset{c}{CH_2}\overset{b}{CH_2}\overset{a}{CH_2}CONH$	H_a, 2.26 (t)	H_a, 0.26 (t)	2.00
	H_b, 2.12 (m)	H_b, −0.11 (m)	2.33
	H_c, 3.37 (t)	H_c, 0.69 (t)	2.68
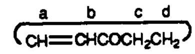 $\overset{a}{CH}{=}\overset{b}{CH}CO\overset{c}{CH_2}\overset{d}{CH_2}$	H_a, 7.70 (m)	H_a, 4.41 (m)	3.29
	H_b, 6.17 (m)	H_b, 3.78 (m)	2.39
	H_c, 2.67 (m)	H_c, 0.51 (m)	2.16
	H_d, 2.32 (m)	H_d, 0.33 (m)	1.99
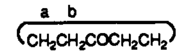 $\overset{a}{CH_2}\overset{b}{CH_2}COCH_2CH_2$	H_a, 1.94 (m)	H_a, 0.38 (t)	1.56
	H_b, 2.15 (m)	H_b, −0.31 (t)	2.46
$C_6\overset{a}{H_6}$	H_a, 7.37 (s)	H_a, 4.70 (s)	2.67
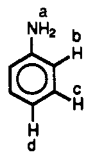	H_a, 3.64 (s)	H_d, −0.34 (s)	3.98
	H_b, 6.69 (d)	H_b, 4.94 (d)	1.75
	H_c, 7.16 (t)	H_c, 5.36 (t)	1.80
	H_d, 6.76 (t)	H_d, 3.02 (t)	3.74
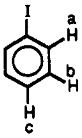	H_a, 7.65 (d)	H_a, 6.65 (d)	1.00
	H_b, 7.40 (t)	H_b, 5.38 (t)	2.02
	H_c, 6.85 (t)	H_c, 3.32 (t)	3.53
$1,4\text{-}Br_2C_6\overset{a}{H_4}$	H_a, 7.29 (s)	H_a, 6.40 (s)	0.89
$1,4\text{-}I_2C_6\overset{a}{H_4}$	H_a, 7.41 (s)	H_a, 6.73 (s)	0.68
$1,4\text{-}(HO)_2C_6\overset{b}{H_4}$	H_a, 7.91 (s)	H_a, 4.62 (s)	3.29
	H_b, 6.72 (s)	H_b, 5.27 (s)	1.45
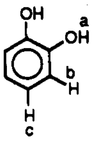	H_a, 5.10 (br)	H_a, 4.00 (s)	1.10
	H_b, 6.85 (m)	H_b, 4.71 (m)	2.14
	H_c, 6.85 (m)	H_c, 4.39 (m)	2.46
$1,4\text{-}(\overset{a}{CH_3})_2C_6\overset{b}{H_4}$	H_a, 2.32 (s)	H_a, −2.08 (s)	4.40
	H_b, 7.07 (s)	H_b, 5.90 (s)	1.17
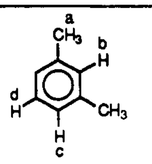	H_a, 2.28 (s)	H_a, −1.04 (s)	3.32
	H_b 6.95 (m)	H_b, 5.55 (s)	1.40
	H_c, 6.95 (m)	H_c, 5.86 (d)	1.09
	H_d, 7.11 (t)	H_d, 5.80 (m)	1.31
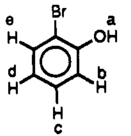	H_a, 5.53 (br s)	H_a, hidden	
	H_b, 7.47 (d)	H_b, 6.30 (d)	1.17
	H_c, 3.13 (t)	H_c, 3.13 (t)	3.67
	H_d, 7.24 (t)	H_d, 6.21 (t)	1.03
	H_e, 7.04 (d)	H_c, 3.77 (d)	3.27
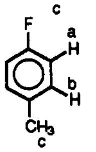	H_a, 6.81 (t)	H_a, 5.65 (t)	1.16
	H_b, 7.00 (d)	H_b, 5.85 (d)	1.15
	H_c, 2.23 (s)	H_c, −1.94 (s)	4.17
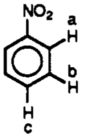	H_a, 8.23 (d)	H_a, 7.04 (d)	1.19
	H_b, 7.55 (t)	H_b, 5.90 (t)	1.65
	H_c, 7.70 (t)	H_c, 3.60 (t)	4.10
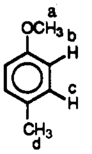	H_a, 3.78 (s)	H_a, −0.35 (s)	4.13
	H_b, 6.81 (d)	H_b, 5.87 (s)	0.94
	H_c, 7.09 (d)	H_c, 5.87 (s)	1.22
	H_d, 2.29 (s)	H_d, −2.11 (s)	4.40
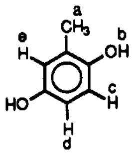	H_a, 2.21 (s)	H_a, −1.72 (s)	3.93
	H_b, 4.31 (s)	H_b, 4.67 (s)	−0.36
	H_c, 6.64 (m)	H_c, 5.84 (s)	0.80
	H_d, 6.64 (m)	H_d, 5.84 (s)	0.80
	H_e, 6.55 (m)	H_e, 5.78 (s)	0.77
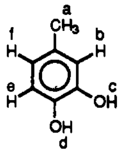	H_a, 2.24 (s)	H_a, −2.21 (s)	4.45
	H_b, 6.70 (s)	H_b, 5.25 (s)	1.45
	H_c, 5.10 (s)	H_c, 4.88 (s)	0.22
	H_d, 4.95 (s)	H_d, 4.88 (s)	0.07
	H_e, 6.75 (d)	H_e, 6.21 (d)	0.54
	H_f, 6.61 (d)	H_f, 5.46 (d)	1.15
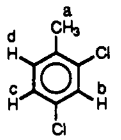	H_a, 2.34 (s)	H_a, −1.47 (s)	3.81
	H_b, 7.35 (s)	H_b, 5.76 (s)	1.59
	H_c, 7.14 (s)	H_c, 5.47 (s)	1.67
	H_d, 7.14 (s)	H_d, 5.47 (s)	1.67
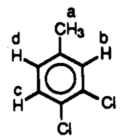	H_a, 2.31 (s)	H_a, −2.15 (a)	4.46
	H_b, 7.26 (s)	H_b, 5.76 (s)	1.50
	H_c, 7.30 (d)	H_c, 6.77 (d)	0.53
	H_d, 7.00 (d)	H_d, 6.22 (d)	0.78
$1,4\text{-}(\overset{a}{CH_3}O)_2C_6\overset{b}{H_4}$	H_a, 3.77 (s)	H_a, −0.46 (s)	4.23
	H_b, 6.86 (s)	H_b, 5.82 (s)	1.03

Thus, the Δδ values for H_i range from 0.25 for C_6H_6, 0.24 for $C_6H_5NO_2$, and 0.24 for one of the two values of 3,4-$Cl_2C_6H_3CH_3$ to −0.12 for one of the two values for C_6H_5I (Table II). Thus, the eight H_i protons on average can reside in either the shielding or deshielding regions of these aromatic guests. Of the non-like-ended aromatic guests, only C_6H_5I, 4-$CH_3C_6H_4OCH_3$, 2,4-$Cl_2C_6H_3CH_3$, and 3,4-$Cl_2C_6H_3CH_3$ display two different sets of H_i and H_a protons in their ^{1}HNMR spectra, which shows that these guests cannot rotate around the short equatorial axis of their host rapidly on the NMR time scale at 25 °C. Being branched, the NO_2 and *p*-H of $C_6H_5NO_2$ as guest cannot be pushed as far into the polar caps as are Cl, I, or CH_3 groups, a posture which should inhibit end-to-end rotation. Even the relatively guest-remote H_p (Ar*H*) signals divide in the spectra of 4-$CH_3C_6H_4OCH_3$, 2,4-$Cl_2C_6H_3CH_3$, and 3,4-$Cl_2C_6H_3CH_3$, whereas the closer H_a (OCH_aO) signals divide in the spectra of all four of these hemicarceplexes. The even more remote host's H_m (Ar_2-RC*H*) signal is least sensitive to the nature of the guest, and its Δδ values never divide and range from +0.01 to −0.09 for all the guests (Table II). The three longest guests, 1,4-$(CH_3O)_2C_6H_4$, 1,4-$I_2C_6H_4$, and 1,4-$CH_3OC_6H_4CH_3$, whose respective CH_3O, I, and CH_3 groups are pushed farthest into the polar caps (model examination), provide the largest Δδ magnitudes (−0.09, −0.07, and −0.06 ppm, respectively).

The protons at the end of the long axes of the guests of classes D–F give the largest Δδ values (ppm) in their ^1H NMR spectra (Table III), which decrease in the following order: 4.46, 3,4-$Cl_2C_6H_3C\mathit{H}_3$; 4.45, 3,4-$(HO)_2C_6H_3C\mathit{H}_3$; 4.40, 1,4-$(C\mathit{H}_3)_2C_6H_4$; 4.23, 1,4-$(C\mathit{H}_3O)_2C_6H_4$; 4.17, 4-$FC_6H_4C\mathit{H}_3$; 4.13, 1,4-$C\mathit{H}_3OC_6H_4CH_3$; 4.10, 1,4-$NO_2C_6H_4\mathit{H}$; 3.98, $\mathit{H}_2NC_6H_5$; 3.93, 2,5-$(HO)_2C_6H_3C\mathit{H}_3$; 3.81, 2,4-$Cl_2C_6H_3C\mathit{H}_3$; 3.67, 2-Br-1,4-$HOC_6H_3\mathit{H}$; 3.53, 1,4-$IC_6H_4\mathit{H}$; and 3.32, 1,3-$(C\mathit{H}_3)_2C_6H_4$. These

Chart I. Stereoviews of Crystal Structures

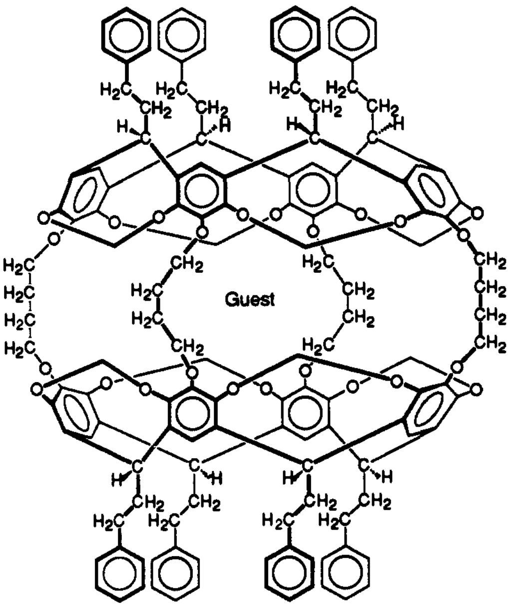

1•Guest

side views

top partial views

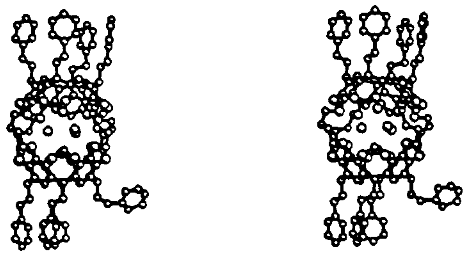

7 ($1 \cdot 6H_2O$)

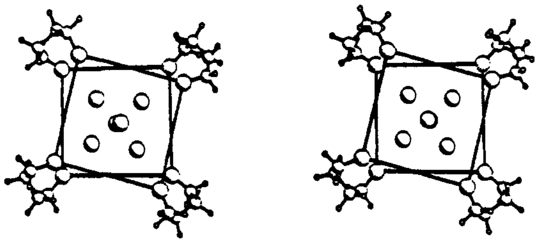

8 ($1 \cdot 6H_2O$)

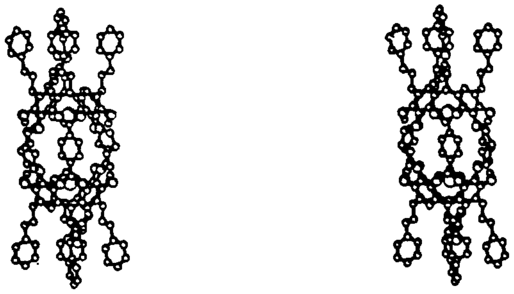

9 ($1 \cdot p\text{-}I_2C_6H_4 \cdot 2C_6H_5NO_2$)

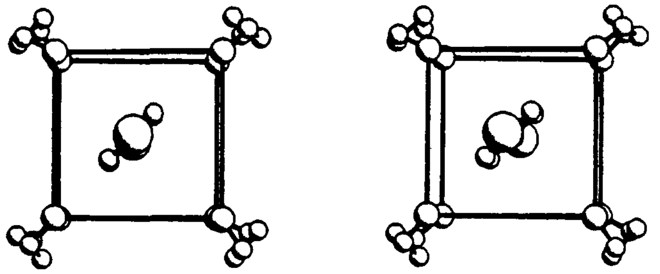

10 ($1 \cdot p\text{-}I_2C_6H_4$)

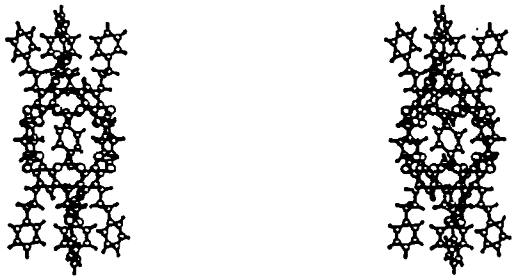

11 ($1 \cdot p\text{-}(CH_3)_2C_6H_4 \cdot 2C_6H_5NO_2$)

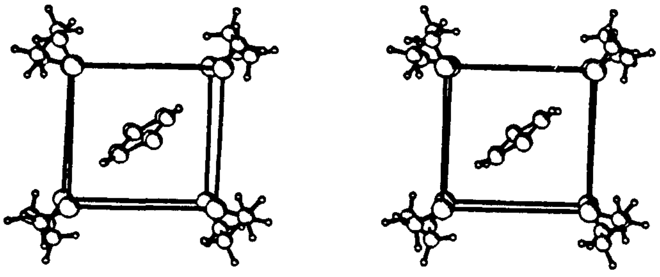

12 ($1 \cdot p\text{-}(CH_3)_2C_6H_4$)

Chart I (Continued)

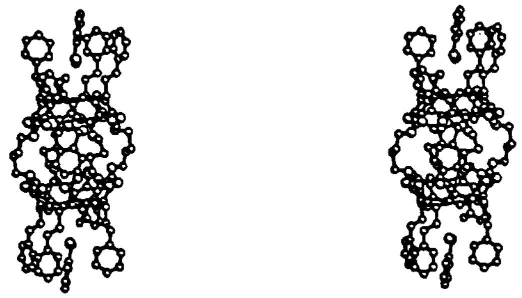

13 ($1\cdot O_2NC_6H_5\cdot 2C_6H_5NO_2$)

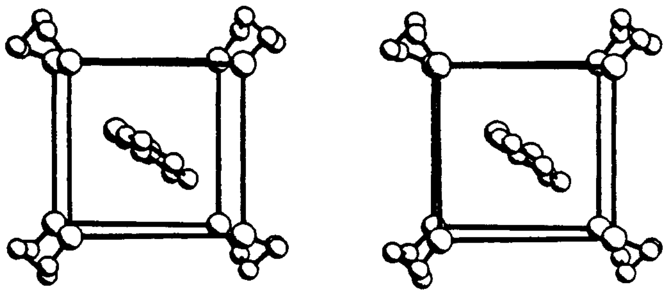

14 ($1\cdot O_2NC_6H_5$)

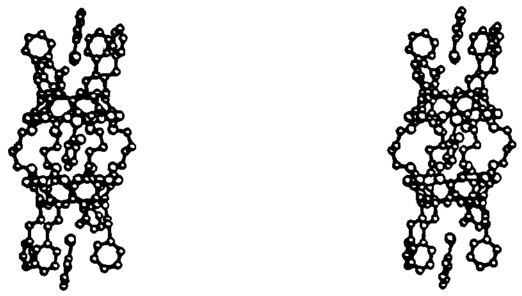

15 ($1\cdot$*o*-$BrC_6H_4OH\cdot 2C_6H_5NO_2$)

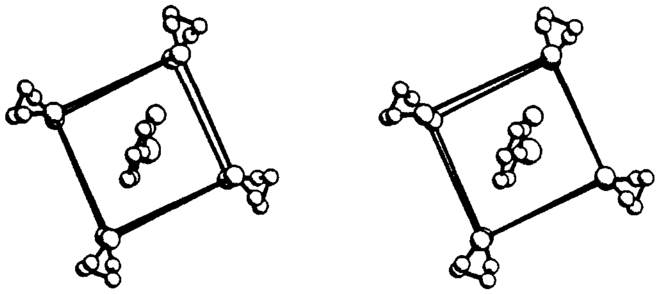

16 ($1\cdot$*o*-BrC_6H_4OH)

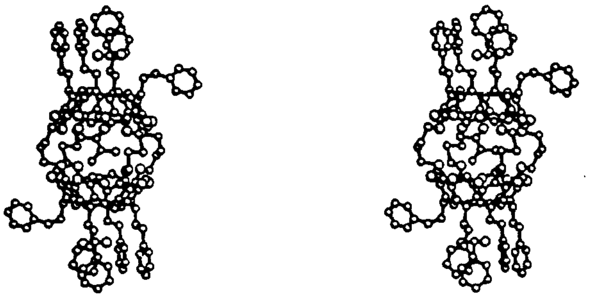

17 ($1\cdot(CH_3)_2NCOCH_3\cdot 2NO_2C_6H_5$)

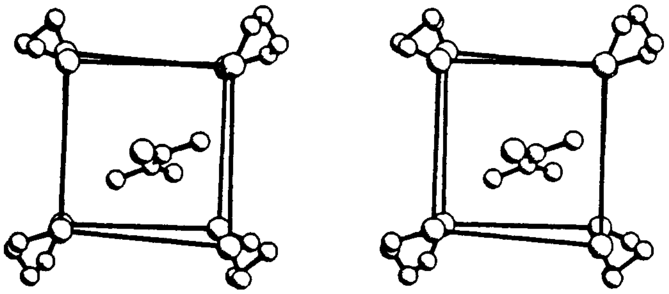

18 ($1\cdot(CH_3)_2NCOCH_3$)

values roughly correlate with the length of the guest's long axis. Model examinations show that one substituent on a guest benzene larger than OH or F inhibits the twisting of the polar caps in the $(BO)_4$ conformation. When two substituents on a guest benzene, such as two methyls or a CH_3 and a halogen, are para to one another, or with one large substituent, such as O_2N or I, very little twisting is possible. Three substituents distributed 1,2,4 to one another are particularly effective in requiring the longest extension of the host along the polar axis.

All of the Ar*H* protons of aromatic guests become shielded upon incarceration, but are the least shielded when locked into the equatorial region of the cavity by large 1,4-substituents rigidly occupying the polar caps. These guests when arranged in increasing order of their ^1H NMR values of $\Delta\delta$ (ppm) for these 2-, 3-, 5- or 6-positioned protons that contain at least 1,4-substituents are as follows (see Table III for proton label): H_c of 3,4-$Cl_2C_6H_3CH_3$, 0.53; H_e of 3,4-$(HO)_2C_6H_3CH_3$, 0.54; H_a of 1,4-$I_2C_6H_4$, 0.68; H_e of 2,5-$(HO)_2C_6H_3CH_3$, 0.77; H_c and H_d of 2,5-$(HO)_2C_6H_3CH_3$, both 0.80; H_a of 1,4-$Br_2C_6H_4$, 0.89; H_b of 4-$CH_3OC_6H_4CH_3$, 0.94; H_b of 1,4-$(CH_3O)_2C_6H_4$, 1.03; H_b and H_a of 4-$FC_6H_4CH_3$, 1.15 and 1.16, respectively. The relatively large O_2N group of $O_2NC_6H_5$ alone is enough to confine its H_a proton to the equatorial region, with $\Delta\delta$ = 1.19 ppm. These $\Delta\delta$ values compare with that of C_6H_6 at 2.67 ppm, which is the averaged degree of shielding for a molecule with considerable freedom of movement.

The crystal structure of $1\cdot$*o*-BrC_6H_4OH shows the Br occupying the polar cap and the OH hydrogen bonded to a proximate ArO of the host, thus placing H_c in the least-shielding equatorial part of the cavity with $\Delta\delta$ = 1.03 ppm. Model examination suggests that most of the phenolic guests are hydrogen bonded to one or another of the host's eight aryl oxygens whose electron pairs are turned inward. The OH protons of these phenolic guests provide $\Delta\delta$ values that increase as follows: –0.36 for H_b of 2,5-$(HO)_2C_6H_3CH_3$; 0.07 and 0.22 for H_c and H_d, respectively, of 3,4-$(HO)_2C_6H_3CH_3$; and 1.10 for H_a of 1,2-$(HO)_2C_6H_4$. The anomalously high value of $\Delta\delta$ for H_a of 1,4-$(HO)_2C_6H_4$ is 3.29. Model examination of $1\cdot$1,4-$(HO)_2C_6H_4$ provided a beautiful structure for this complex in which the guest is slung like a hammock across the cavity, being held at one end by a hydrogen bond to an ArO of one hemisphere and to a second and opposite ArO of the other hemisphere.

Structural Recognition during Complexation. Although no kinetics of complexation were examined, qualitative conclusions can be drawn from the times, temperatures required for complexation, and inadvertent competition experiments that were conducted. Clearly, the small open-chain guests of class A, with the exception of $(CH_3)_2NCOCH_3$, complex **1** more readily than the five-membered ring cycles of class B, which in turn complex more readily than the monosubstituted benzenes of class C. Of the members of this last series, $C_6H_5NO_2$ complexed **1** less readily than the other members of the class, being more comparable to

Chart II

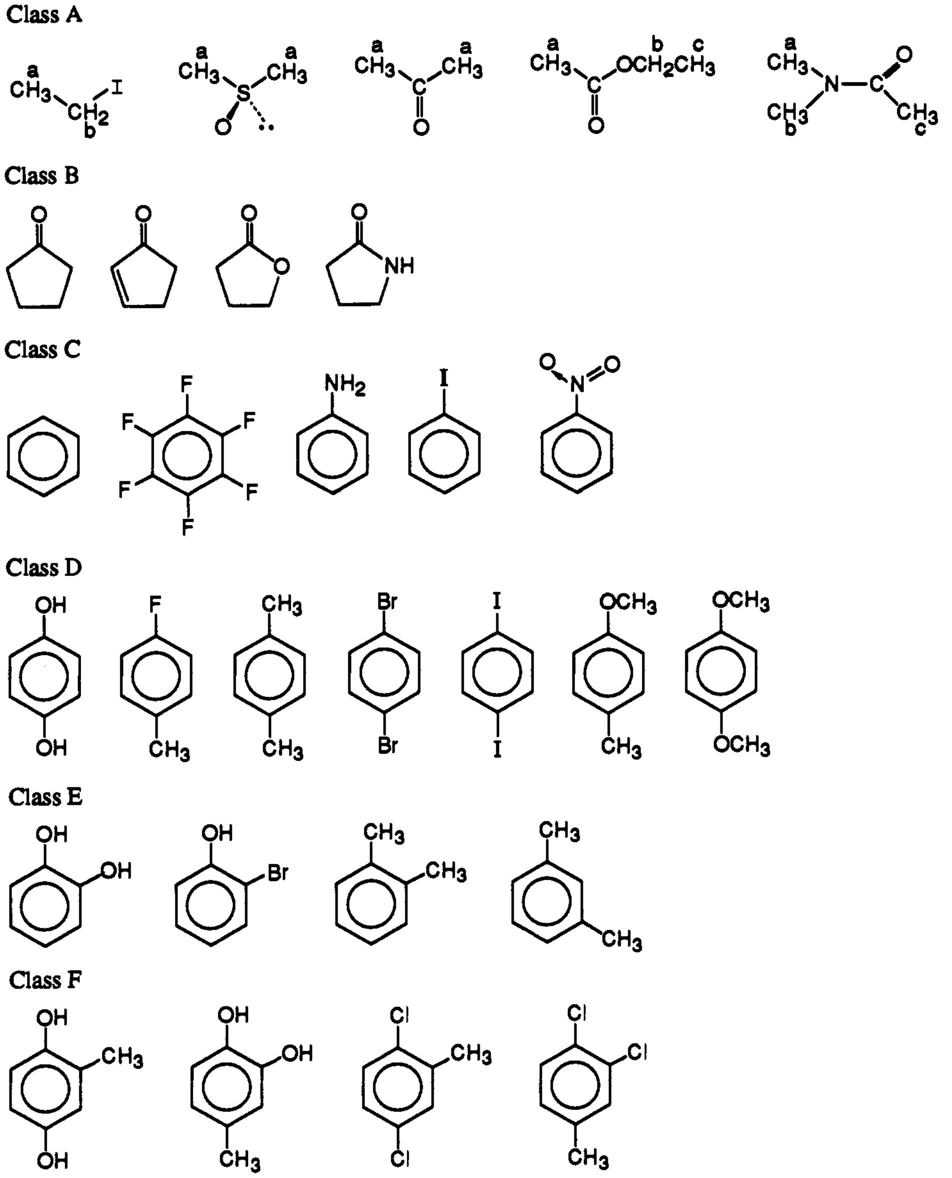

the 1,4-disubstituted benzenes of 1 class E, whose most easily complexed member was 1,4-$(HO)_2C_6H_4$. Generally, one or two hydroxyl groups attached to a benzene made complexation somewhat easier. Generally, 1,4-disubstituted isomers were complexed more readily than 1,3-disubstituted, which in turn were complexed more readily than 1,2-disubstituted isomers of class E.

An interesting example of the last generalization involved an inadvertent competition experiment. When an attempt was made to incarcerate *o*-xylene into empty **1**, 98% HPLC grade *o*-xylene (Aldrich) containing dissolved **1** was heated to reflux at ~140 °C for 4 days. A mixture of **1**·*o*-xylene, **1**·*m*-xylene, and **1**·*p*-xylene was formed in which **1**·*p*-xylene dominated (^1H NMR spectral measurements). When **1** was refluxed (~140 °C) in 99+% anhydrous *m*-xylene (Aldrich), a 2:1 mixture of **1**·*m*-xylene to **1**·*p*-xylene was produced. When **1** was refluxed in certified *p-xylene (Fisher), only* **1**·*p*-xylene was obtained. Obviously, *p*-xylene ≫ *m*-xylene > *o*-xylene in their rate constants for complexation. These results exemplify the high structural recognition that **1** shows toward constitutional isomers with widely differing shapes but identical bulk and molecular parts.

Class F guest compounds, particularly the two dichlorotoluene isomers, entered the interior of **1** with the greatest difficulty, as would be expected from model examination. In a number of cases, attempts to obtain di- and trisubstituted benzene complexes were defeated by the presence in the guest of impurities that entered the host more rapidly than the major component present. Examples involved impure 1,2-$(CH_3O)_2C_6H_4$ and 1,2,4-$Cl_3C_6H_3$, which were employed as solvent.

Decomplexation. Decomplexation rates were on the human time scale at temperatures around 100 °C for all guests of class A except for $(CH_3)_2NCOCH_3$, whose decomplexation first-order rate constants were determined in $C_6D_5NO_2$ at 140, 150, 160, and 170 °C to provide an E_a value of 23.5 ± 1.5 kcal mol^{-1}. At these temperatures the rate of complexation of $C_6D_5NO_2$ is very slow. This value is high enough to demonstrate that much of the total activation free energy for decomplexation of **1**·$(CH_3)_2NCOCH_3$ is constrictive, which adds to the intrinsic binding to provide the complex with high stability at working temperatures.[3] Although we have no quantitative comparisons between the hosts **1** and **3** in their abilities to retain the same guest in the same solvent at the same temperature, the many preliminary qualitative experiments coupled with those reported here leave little doubt that **3**·guests in general decomplex more easily (temperature and time) than does the **1**·guest family of hemicarceplexes. There are many more degrees of conformational freedom and eight more hydrogens that line the cavity in the $(OCH_2CH_2CH_2CH_2O)_4$ bridges of **1** than in those of the (1,2-$OCH_2C_6H_4CH_2O)_4$ bridges of **3**. The latter factor should slow the rate of both entrance and release of guests into **1** as compared to **3**, but the former factor

Table IV. Interesting Host Angles (deg) in Crystal Structures of Seven Hemicarceplexes

	angles (°)		
complex	twist around polar axis	dihedral between Ar[a] and Ar–O–C planes	Ar–O–C[a] bond angles
$\mathbf{1}\cdot 6H_2O$	15	81 ± 4	113 ± 2
$\mathbf{1}\cdot p\text{-}I_2C_6H_4$	1	70 ± 6	115.3 ± 0.3
$\mathbf{1}\cdot p\text{-}(CH_3)_2C_6H_4$	0	56 ± 9	104 ± 8
$\mathbf{1}\cdot O_2NC_6H_5$	0	71 ± 6	114.5 ± 1
$\mathbf{1}\cdot o\text{-}BrC_6H_4OH$	1	57 ± 8	115 ± 4
$\mathbf{1}\cdot (CH_3)_2NCOCH_3$	0	65 ± 6	126 ± 10
$\mathbf{3}\cdot$guest[b]	21	74 ± 6	107 ± 6

[a] Benzenes are assumed to be planar. [b] Data taken from ref 3; guest is unknown.

might operate in either direction. Without doubt, **1** complexes strongly a much larger family of guests than **3**, whose largest guest was $p\text{-}(CH_3)_2C_6H_4$ and whose smallest was $CH_3C{\equiv}N$. Generally, the FABMS of **1**·guest signals were much stronger compared to those for **1** than was observed for **3**·guest vs **3**, suggesting that the above generalization of greater stability for complexes of **1** compared to **3** also applies to the gas as well as to the liquid phase.

Crystal Structures. Chart I contains side stereoviews **7, 9, 11, 13, 15,** and **17** and the corresponding top partial stereoviews **8, 10, 12, 14, 16,** and **18** of $\mathbf{1}\cdot 6H_2O$, $\mathbf{1}\cdot I_2C_6H_4\cdot 2C_6H_5NO_2$, $\mathbf{1}\cdot p\text{-}(CH_3)_2C_6H_4\cdot 2C_6H_5NO_2$, $\mathbf{1}\cdot O_2NC_6H_5\cdot 2C_6H_5NO_2$, $\mathbf{1}\cdot o\text{-}BrC_6H_4OH\cdot 2C_6H_5NO_2$, and $\mathbf{1}\cdot (CH_3)_2NCOCH_3\cdot 2C_6H_5NO_2$, respectively. In the top views (along the polar axis), the northern and southern bowls have been replaced by the near squares formed by connecting the two sets of four oxygens that terminate each end of the four $O(CH_2)_4O$ bridging groups. These stereoviews unequivocally establish the presence in the interior of **1** of six H_2O in **7** and **8**, $p\text{-}I_2C_6H_4$ in **9** and **10**, $p\text{-}(CH_3)_2C_6H_4$ in **11** and **12**, $O_2NC_6H_5$ in **13** and **14**, $o\text{-}BrC_6H_4OH$ in **15** and **16**, and $(CH_3)_2NCOCH_3$ in **17** and **18** as guests. In the latter five systems, two $C_6H_5NO_2$ molecules fill the cavitand-like void created by the two sets of four $C_6H_5CH_2CH_2$ appendages, with the nitro groups closest to the globe-shaped body of the host. These five latter complexes belong to the same space group ($P2_1/c$) and possess similar shapes and volumes (at 25 °C), the latter ranging from 6895 Å^3 for $\mathbf{1}\cdot o\text{-}I_2C_6H_4\cdot 2C_6H_5NO_2$ to 6799 Å^3 for $\mathbf{1}\cdot (CH_3)_2NCOCH_3\cdot 2C_6H_5NO_2$. The host of these six complexes is in each case centrosymmetric, whereas complexes $\mathbf{1}\cdot p\text{-}I_2C_6H_4\cdot 2C_6H_5NO_2$ and $\mathbf{1}\cdot p\text{-}(CH_3)_2C_6H_4\cdot 2C_6H_5NO_2$ as a whole are centrosymmetric. The polar axes of the host and guest are collinear in $\mathbf{1}\cdot p\text{-}I_2C_6H_4$ and $\mathbf{1}\cdot p\text{-}(CH_3)_2C_6H_4$. The angles of twist of the polar caps around the polar axis are listed in Table IV (along with other hemicarceplex angles). The former is essentially 0 for all complexes but $\mathbf{1}\cdot 6H_2O$, as is visible in **10, 12, 14, 16,** and **18**. Important from the point of view of generating maximum cavity sizes, all of the $O(CH_2)_4O$ bridges are located outside that part of the cavity defined by the oxygen squares of **8–18**. We interpret this as reflecting a tendency of the unshared electron pairs of the oxygens terminating the four bridges to face inward to compensate somewhat in each case for the dipoles created by the unshared electron pairs of the two flanking oxygens facing outward. The latter possesses this conformation, which is enforced by the shortness of the eight intrahemispheric OCH_2O bridges. The dihedral angles between the aryl planes and the COC plane of the ArOC moieties range from 81° to 56° for the six hemicarceplexes, while the COC bond angles of the same moieties range from 113° to 126° (Table IV), the longest guest ($p\text{-}I_2C_6H_4$) requiring the largest opening of this angle. The angle of twist of the two hemispheres in $\mathbf{1}\cdot 6H_2O$ is 15° (see **8** of Chart I), which is the complex of **1** with the smallest Ar–O–C bond angle (113°). The twist angle of $\mathbf{1}\cdot 6H_2O$ is still less than that for **3**·guest at 21°, whose guest was not identified. That this guest is highly complementary to the cavity is also suggested by the ArOC bond angle of **3**·guest being next to the smallest of the seven complexes of Table IV at 107°. Molecular models of empty **1** suggest that hemicarceplexes containing small guests such as CH_3CH_2I or CH_3COCH_3 possess twisted conformations.

The cavity sizes and shapes of host **1** can be usefully described in terms of the parameters taken from the six crystal structures of **1**·guest and that of **3**·guest listed in Table V. Each of the host cavities is composed of six roughly parallel square cross sections stacked perpendicularly to the polar axis. The six squares of the globe are defined from south to north by the following sets of four atoms: southern aryl polar carbons (bonded to hydrogens); southern aryl oxygens of the interhemispheric bridges; southern equatorial carbons of the C–*C*–C–C bridges; northern equatorial carbons of the C–C–*C*–C bridges; northern aryl oxygens of the bridges; and the northern polar aryl carbons (bonded to hydrogens). The distances between selected pairs of these planes are provided in Table V. The effective polar length of the cavities approximately equals the distance between the north and south polar carbon planes minus the diameter of a covalently bonded carbon for each complex (1.54 Å). These lengths in decreasing order of magnitude in angstroms are as follows: $\mathbf{1}\cdot I_2C_6H_4$, 10.27; $\mathbf{1}\cdot p\text{-}(CH_3)_2C_6H_4$, 9.89; $\mathbf{1}\cdot o\text{-}BrC_6H_4OH$, 9.67; $\mathbf{1}\cdot O_2NC_6H_5$, 9.60; $\mathbf{1}\cdot (CH_3)_2NCOCH_3$, 9.57; $\mathbf{1}\cdot 6H_2O$, 9.01; **3**·guest, 8.14. These distances compare with the long-axis lengths of the guests in CPK molecular models (Å) as follows: $p\text{-}I_2C_6H_4$, 10.35; $p\text{-}(CH_3)_2C_6H_4$, 8.5; $o\text{-}BrC_6H_4OH$, 8.61; $O_2NC_6H_5$, 8.2; $(CH_3)_2NCOCH_3$, 7.2. Thus, the cavity length in $\mathbf{1}\cdot p\text{-}I_2C_6H_4$ is 0.08 Å shorter than the guest model length, which is within about 1% of a fit in this dimension. The other guests of **1** are substantially shorter in their longest dimension than the cavity of the host taken from the crystal structures. As expected, the cavities of the twisted complexes $\mathbf{1}\cdot 6H_2O$ and **3**·guest are ~10% and ~20% shorter than the untwisted cavities.

The distances between the two central O's planes in the complexes range from 4.14 Å in $\mathbf{1}\cdot p\text{-}I_2C_6H_4$ to 3.12 Å in $\mathbf{1}\cdot 6H_2O$, the decrease again reflecting the twisting of the hemispheric caps, which in **3**·guest at 21° decreases the distance to 2.34 Å. The short distances between the two central carbon planes range between only 0.04 and 0.49 Å in the four complexes of **1**, but the distance increases to 1.13 Å in the highly twisted **3**·guest, which contains $o\text{-}CH_2C_6H_4CH_2$ bridges.

The maximum diameters of the cavities are best measured by the diagonals of the two squares of the oxygens minus the diameter of a covalently bound oxygen (2.80 Å). The resulting values are as follows (Å): **3**·guest, 6.32; $\mathbf{1}\cdot p\text{-}(CH_3)_2C_6H_4$, 6.26; $\mathbf{1}\cdot 6H_2O$, 6.18; $\mathbf{1}\cdot o\text{-}BrC_6H_4OH$, 6.16; $\mathbf{1}\cdot (CH_3)_2NCOCH_3$, 6.16; $\mathbf{1}\cdot O_2NC_6H_5$, 6.12; $\mathbf{1}\cdot p\text{-}I_2C_6H_4$, 5.84. As is intuitively obvious, the longer the cavity of **1** (e.g. 10.26 Å in $\mathbf{1}\cdot p\text{-}I_2C_6H_4$), the narrower the cavity (5.84 Å). The shorter the cavity of **1** (e.g. 9.01 Å in $\mathbf{1}\cdot 6H_2O$), the wider the cavity (6.18 Å). The fact that the spread is small testifies to the overall rigidity of the cavity. A further measure of the cavities' insensitivity to guest dimensions and even to interhemispheric bridges is found in the low spread of values of diagonal distances between coplanar oxygens of the OCH_2O variety. These distances vary only from 9.29 ± 0.03 Å in $\mathbf{1}\cdot o\text{-}BrC_6H_4OH$ to 9.46 ± 0.07 Å in **3**·guest, the values for the other complexes lying between these two.

Table V also contains the distances the ArO's O atoms are bent inward from the Ar plane. The longest of these distances is only 0.25 Å and is found in $\mathbf{1}\cdot p\text{-}I_2C_6H_4$, whose guest requires a cavity of maximum length. The shortest is 0.06 Å, found in $\mathbf{1}\cdot p\text{-}(CH_3)_2C_6H_4$, whose polar length is substantially less than that of the cavity. The next shortest is 0.13 Å, found in $\mathbf{1}\cdot 6H_2O$, whose composite guest is the shortest in polar length.

Molecular models of $\mathbf{1}\cdot o\text{-}BrC_6H_4OH$ indicate that when the Br atom is inserted firmly into a polar cap, the OH group is in a position to hydrogen bond an $ArOCH_2CH_2$'s oxygen. Side view **13** of the crystal structure of this complex shows that such a host–guest hydrogen bond exists, the relevant O···O distance being 3.3 Å.

Table V. Interesting Host Distances (Å) in Crystal Structures of Seven Hemicarceplexes

		O–C–C–C–C–O bridges				
		distance between best planes				
complex	distances, bottom to top of C's planes	two central O's planes	two central C's planes	diagonal O's distance	OCH_2O bridges, diagonal O's distances	distance, ArO's O to Ar plane
$1{\cdot}6H_2O$	10.55 ± 0.11	3.12 ± 0.16	0.47 ± 0.06	8.98 ± 0.11	9.35 ± 0.05	0.13 ± 0.025
$1{\cdot}p\text{-}I_2C_6H_4$	11.81 ± 0.01	4.14 ± 0.02	0.47 ± 0.12	8.64 ± 0.03	9.32 ± 0.06	0.25 ± 0.05
$1{\cdot}p\text{-}(CH_3)_2C_6H_4$	11.43 ± 0.01	3.94 ± 0.01	0.45 ± 0.01	9.06 ± 0.06	9.34 ± 0.11	0.06 ± 0.06
$1{\cdot}O_2NC_6H_5$	11.14 ± 0.20	3.82 ± 0.04	0.49 ± 0.03	8.92 ± 0.04	9.36 ± 0.03	0.22 ± 0.03
$1{\cdot}o\text{-}BrC_6H_4OH$	11.21 ± 0.03	3.82 ± 0.02	0.47 ± 0.01	8.96 ± 0.13	9.29 ± 0.03	0.18 ± 0.06
$1{\cdot}(CH_3)_2NCOCH_3$	11.11 ± 0.03	3.63 ± 0.03	0.04 ± 0.03	8.96 ± 0.02	9.31 ± 0.11	0.19 ± 0.04
3·guest	9.68 ± 0.06	2.34 ± 0.08	1.13 ± 0.52	9.03 ± 0.18	9.46 ± 0.07	0.15 ± 0.06

Scheme I. Top View of Octahedrally Arranged $6H_2O$ Guests Held Together by Six Hydrogen Bonds, the Octahedron Anchored by Six Hydrogen Bonds to the Eight Most Equatorially Located Oxygens of the Host Twisted 15°[a]

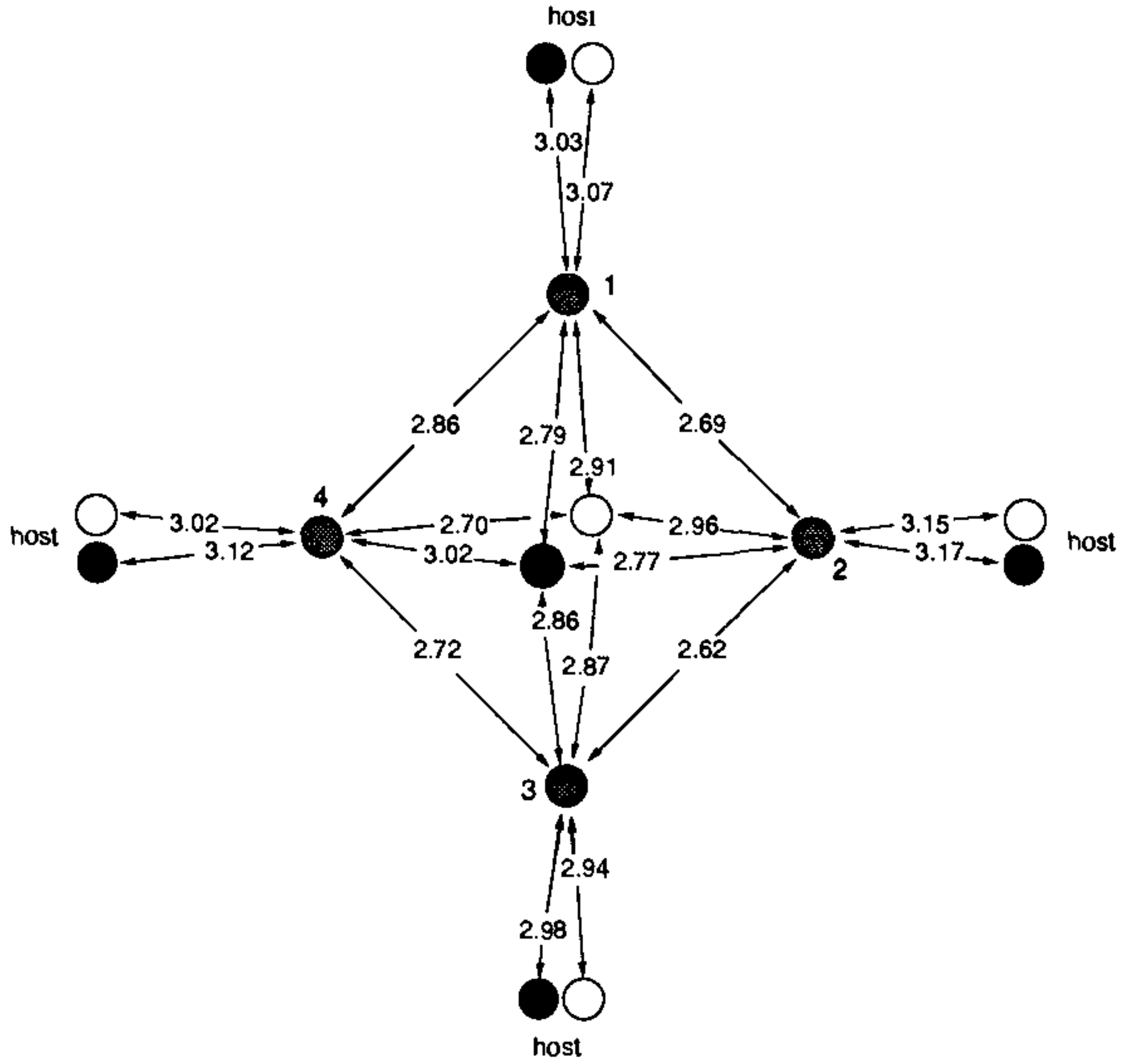

[a] The O···O distances are indicated in angstroms. The black oxygens are above the plane of the page, the gray ozygens are in that plane, and the white oxygens are below the plane of the page.

Interesting Guest Structure in $1{\cdot}6H_2O$. This complex formed from "empty 1" after guest had been driven out by heating at 200 °C dissolved in Ph_2O for days. One sample thus prepared of "empty 1" gave elemental analysis for $1{\cdot}H_2O$ and a second for $1{\cdot}2H_2O$. This latter sample when slowly crystallized from $o\text{-}(CH_3)_2C_6H_4$ gave crystals of $1{\cdot}6H_2O{\cdot}4o\text{-}(CH_3)_2C_6H_4$, which was submitted to crystal structure determination to give $R = 0.15$, with the $o\text{-}(CH_3)_2C_6H_4$ solvate molecules being partially disordered and located near the feet and between the molecules of the complex. Thus, "empty 1" slowly accumulated its six water guests over time into the irregular octahedral structure, which is particularly visible in top stereoview 8 of Chart I. We have no proof that the six positions of the octahedron are all occupied all of the time, but there is no doubt about the approximate octahedral arrangement of the oxygens. The 15° twist of the two hemispheric bowls does not alter the collinearity of the host's polar axis with the octahedral axis of the guest. The hydrogens of the six H_2O guest molecules were not located.

In CPK molecular models, crystal structure 7 can be readily assembled in which six H_2O molecules are hydrogen bonded to one another and to the host as follows. The four equatorial waters form a square held together by hydrogen bonds between oxygens, the four remaining hydrogens being hydrogen bonded to the host's eight equatorial oxygens. The remaining two H_2O molecules, each located in one of the two polar caps, donate hydrogen bonds to unshared electron pairs of diagonally-located equatorial oxygens. This arrangement is complementary to the *roughly octahedral shape of the inner phase of empty 1.* In this model, the hydrogen bonds from the guest to the host are either bifurcated or averaged.

Table VI. Distances between Close Oxygens of Guest and between Host–Guest Close Oxygens, and Bonding Angles between O···O···O of Guest in $1{\cdot}6H_2O$

kind of O···O	number	distance (Å)
equatorial–equatorial	4	2.72 ± 0.07
equatorial–axial	8	2.86 ± 0.08
host to equatorial guest	8	3.06 ± 0.08
guest axial to axial	1	4.24

O_e of $O{\cdots}O_e{\cdots}O$	number	angle (deg)
0–1	5	107 ± 8
0–2	6	104 ± 8
0–3	8	110 ± 13
0–4	5	106 ± 9

This CPK model of **1**·$6H_2O$ nicely accommodates the crystal structure whose guest and host oxygens and their close O···O distances are viewed in Scheme I and averaged in Table VI. Table VI also provides the O···O_e···O averaged bond angles in which the O_e oxygens are the four equatorial oxygens of the $6H_2O$ guest.

The four equatorial oxygens of the guest provide a crude square whose close O···O distances range from 2.70 to 3.02 Å (Scheme I) and average 2.72 ± 0.07 Å (Table VI). The eight equatorial to axial O···O distances range from 2.62 to 2.91 Å (Scheme I), to provide an average of 2.86 ± 0.08 Å. The eight equatorial host–guest O···O distances range from 2.94 to 3.17 Å (Scheme I) and average 3.06 ± 0.08 Å. Since there are 12 hydrogens to be distributed between these 16 close pairs of oxygens and they are likely located between the closest 8 O···O distances, the 8 longer O···O host–guest oxygens must share the remaining 4 hydrogens, either by forming bifurcated hydrogen bonds or by averaging one hydrogen bond between two possible oxygen pairs. The guest axial-to-axial O···O distance is 4.24 Å, which if added to the diameter of a covalently bonded oxygen (2.80 Å), gives 6.04 Å for the length of the polar axis of the octahedral and composite guest, well within the 9.01-Å length along the polar axis of the cavity.

Table VI also gives averages for the O···O_e···O bond angles in which O_e is one of the four (numbered 1–4 in Scheme I) equatorial oxygens, as well as the number of angles averaged. The extremes of the angles averaged were 93° and 132°. Notice that the four averages range from 104° to 110°.

The O···O distances and the O···O···O bond angles in incarcerated $6H_2O$ provide interesting comparisons to the values exhibited by the various forms of ice.[9] In ordinary ice (ice I, hexagonal) at 0 °C and atmospheric pressure, each oxygen atom is at the center of a tetrahedron formed by four oxygen atoms, each about 2.76 Å distant. Each water molecule is hydrogen bonded to its four nearest neighbors, providing an open lattice of lower density than water. The dimensions of a molecule of water in ice I are nearly the same as those of an isolated molecule: the O–H bond length is 1.01 Å, and the H–O–H bond angle is not much greater than the 104.5° of an isolated molecule. The O···O···O bond angles are 109.5°.[6]

These values are close to the overall averages found in the $6H_2O$ guest. The O···O close distances are 2.81 Å in $6H_2O$ guest vs 2.76 Å for ice I. The O···O_e···O bond angles in $6H_2O$·8O (equatorial of host) average overall 107° vs 109.5° for ice I. These differences are generally comparable to those found among the I–VIII polymorphs of ice.[9]

Summary. A new hemicarceplex has been synthesized around a $(CH_3)_2NCOCH_3$ molecule as guest, **1**·$(CH_3)_2NCOCH_3$, which has been liberated (Ph_2O as solvent) at 195 °C to give empty **1**. Twenty-nine different organic molecules and Xe were heated into **1** at temperatures from 57 to 195 °C to form 1:1 complexes that are stable under ambient conditions, the complexation being driven by mass law and intrinsic binding, and distributing the single empty space inside the carcerand into many smaller empty spaces throughout the medium (entropy of dilution of space).[3] The guests range in size from Xe to CH_3CH_2I to *p*-$(CH_3)_2C_6H_4$ and 3,4-$Cl_2C_6H_3CH_3$. Constrictive binding contributes strongly to the kinetic stability of these hemicarceplexes. Generally *p*-$X_2C_6H_4$ ≫ *m*-$X_2C_6H_4$ > *o*-$X_2C_6H_4$ in ease of complex formation and decomplexation at high temperatures. These complexes give strong FABMS $m/e = M^+ + 1$ signals as the parent ion and ^1H NMR spectra which distinguish whether nonlike-ended guests could rotate rapidly on the NMR time scale at ambient temperature. Crystal structures of **1**·$6H_2O$, **1**·*p*-$I_2C_6H_4$, **1**·*p*-$(CH_3)_2C_6H_4$, **1**·$O_2NC_6H_5$, **1**·*o*-BrC_6H_4OH, and **1**·$(CH_3)_2NCOCH_3$ were determined. In **1**·$6H_2O$, the six waters are strongly hydrogen bonded to one another and form an octahedron, anchored within the octahedral cavity to eight inward-turned $O(CH_2)_4O$ oxygens of the host that line the equatorial region of the cavity. The close O···O oxygen distances and the O···O_e···O bond angles average to values in the same range as those in the eight polymorphic forms of ice. The other five crystal structures appear to be isomorphous, responding to different guest shapes and sizes only in minor ways. Complex **1**·$6H_2O$, unlike the other five, is twisted around the polar axis 15°, which generates more intrahemisphere and bridge close contacts. This host is the strongest and most versatile binding hemicarcerand yet prepared.

Experimental Section

General. All chemicals were reagent grade and used directly unless otherwise specified. All reactions were conducted under argon unless otherwise noted. Tetrahydrofuran (THF) was freshly distilled from sodium benzophenone ketyl just prior to use. Dimethyl acetamide (DMA) and dimethyl sulfoxide (DMSO) were stored over (24 h heated at 320 °C) 3-Å molecular sieves and degassed under high vacuum just before use. In all procedures involving $CHCl_3$ with uncomplexed **1**, the solvent was passed through a plug of silica gel prior to use to remove EtOH. A Bruker AM 500-MHz spectrometer was used to record ^1H NMR spectra unless otherwise noted. Spectra taken in $CDCl_3$ were referenced to residual $CHCl_3$ at 7.26 ppm. Spectra taken in $CDCl_2CDCl_2$ were referenced to $CHCl_2CHCl_2$ at 5.99 ppm. NMR samples that were saturated with a gas (Xe) were prepared by passing a stream of that gas through the sample for a minimum of 10 min. Degassed NMR samples were prepared by freezing the samples in liquid nitrogen, evacuating to 0.1 Torr, and thawing three times before sealing. FABMS were determined on a ZAB SE instrument with 3-nitrobenzyl alcohol (NOBA) as a matrix. Gravity chromatography was performed on E. Merck silica gel 60 (70–230 mesh). Thin-layer chromatography involved glass-backed plates (silica gel 60, F_{245}, 0.25 mm).

34,47-(Epoxybutanoxy)-20,24:57,61-dimethano-2,52:17,29-dimetheno-3,51,16,30-(methynoxybutanoxymethyno)-1*H*,18*H*,26*H*,28*H*,53*H*,55*H*-bis[1,3]benzodioxocino[9,8-*d*:9′,8′-*d*′]bis[1,3]benzodioxocino[9′,10′:17,18;10″,9″:25,26][1,3,6,11,14,16,19,24]octaoxacyclohexacosino[4,5-*j*:13,12-*j*′]bis[1,3]benzodioxocin, 8,9,10,11,39,40,41,42-Octahydro-1,18,26,28,53,55,63,80-octakis(2-phenylethyl)-, Stereoisomer, $(CH_3)_2NCOCH_3$ Complex [1·$(CH_3)_2NCOCH_3$], Procedure A. To a heated (60 °C) stirred mixture of 8 g of Cs_2CO_3 and 500 mL of degassed DMA under a blanket of argon were added 1.0 g (1.0 mmol) of tetrol **5**[6] and then by a syringe pump a solution of 1,4-butanediol ditosylate dissolved in 70 mL of degassed DMA over a period of 2 days. An additional amount of 0.8 g (2.0 mmol) of ditosylate was added, and stirring was continued at 60–70 °C for 2 days. The mixture was cooled to 25 °C, and the solvent was evaporated in vacuo. The residue was dissolved in $CHCl_3$ and filtered through a 1-cm pad of Celite. Again the solvent was evaporated in vacuo, and the residue was chromatographed on a column of silica gel with CH_2Cl_2 as the mobile phase to give 300 mg (30%) of **1**·$(CH_3)_2NCOCH_3$: ^1H NMR (360 Hz, $CDCl_3$), δ −1.64 (s, 3H, CH_3-CO), −1.42 (s, 3H, NCH_3 *cis* to C═O), 1.61 (s, 3H, NCH_3 *trans* to C═O), 2.00 (br s, 16H, OCH_2CH_2), 2.49 (m, 16H, $CH_2CH_2C_6H_5$), 2.68 (m, 16H, $CH_2CH_2C_6H_5$), 3.92 (br s, 16H, OCH_2CH_2), 4.29 (d, 8H, J = 7.2 Hz, inner OCH_2O), 4.84 (t, 8H, J = 7.2 Hz, methine), 5.81 (d, 8H, J = 7.2 Hz, outer OCH_2O), 6.84 (s, 8H, Ar*H* of hemisphere), 7.15 (m, Ar*H* on feet), 7.23 (s, 24H, Ar*H* on feet); FABMS, NOBA, Xe, m/e (2337.8) 2338 (100) 2249.1 (30). Anal. Calcd for $C_{148}H_{145}NO_{25}$ (2337.8): C, 76.04; H, 6.25; N, 0.60. Found: C, 76.23; H, 6.14; N, 0.43.

"Empty 1". Into a Pyrex test tube capped with a rubber septum were placed 154.1 mg (0.066 mmol) of **1**·$(CH_3)_2NOCH_3$ and 5 mL of pure Ph_2O. This mixture was heated at 195 °C for 5 days. The mixture was cooled and poured into 50 mL of MeOH, and the precipitate was filtered and washed with MeOH to give 140 mg (94%) of "empty **1**" after drying. If dark brown in color, this material in CH_2Cl_2 was passed through a short silica gel–CH_2Cl_2 column to give **1**, which was dried at 80 °C under high vacuum; ^1H NMR (500 MHz, $CDCl_3$) δ 2.01 (br s, 16H, OCH_2CH_2), 2.50 (m, 16H, $CH_2CH_2C_6H_5$), 2.69 (m, 16H, $CH_2CH_2C_6H_5$), 3.92 (br s, 16H, OCH_2CH_2), 4.30 (br d, 8H, inner OCH_2O), 4.82 (t, 8H, J = 7.5 Hz, methine), 5.81 (d, 8H, outer OCH_2O, J = 5.0 Hz), 6.85 (s, 8H, Ar*H* on hemisphere), 7.16 (m, 16H, Ar*H* on feet), 7.23 (s, 24H, Ar*H* on feet); FABMS (Xe, NOBA) m/e (2250.6) 2251.3 (100), 2160.3 (10). Anal. Calcd for $C_{144}H_{136}O_{24}$·$2H_2O$ (2286.7): C, 75.64; H, 6.17. Found: C, 75.42; H, 6.00. In a second preparation of "empty **1**", only one molecule of H_2O was found in the host (see Tables I–III for analytical, MS, and ^1H NMR data).

---

[9] Eisenberg, D.; Kauzmann, W. *The Structure and Properties of Water*; Oxford University Press: New York, 1969; p 85.

Application of procedure A to 8 g of Cs_2CO_3, 800 mL of degassed $(CH_3)_2SO$, 1 g of tetrol **5**, and a total of 3.2 g of 1,4-butanediol ditosylate after 4 days at 60–70 °C gave, after chromatography of the product, 200 mg (20%) of **1**·$(CH_3)_2SO$ (see Tables I–III for characterization). This is procedure B.

36,51-(Epoxybutanoxy)-22,26:61,65-dimethano-2,56:19,31-dimetheno-3,55,18,32-(methynoxybutanoxymethyno)-1*H*,20*H*,28*H*,30*H*,57*H*,59*H*-bis[1,3]benzodioxocino[8,9:21,22]bis[1,3]benzodioxocino[9′,10′:17,18:10″,9″:25,26][1,3,6,11,14,16,19,24]octaoxacyclohexacosino[4,5-*j*;13,12-*j*′]bis[1,3]benzodioxocin, 8,13,41,46-Tetrahydro-1,20,28,30,57,59,67,92-octakispentyl-, Stereoisomer, $(CH_3)_2SO$ Complex [2$(CH_3)_2SO$]. Application of procedure B to 3 g of Cs_2CO_3, 300 mL of degassed $(CH_3)_2SO$, 230 mg (0.26 mmol) of tetrol **6**,[4] a total of 0.84 g (2.1 mmol) of 1,4-butanediol ditosylate (3 portions) was added by syringe pump (high dilution) over a total of 5 days at 60–70 °C. The solvent was removed in vacuo, and the residue was dissolved in $CHCl_3$ and filtered through a 1-cm pad of Celite. The solvent was evaporated in vacuo and the residue chromatographed on silica gel with 1% EtOAc (v) in CH_2Cl_2 as the mobile phase to give 40 mg (18%) of **2**·$(CH_3)_2SO$: FABMS, NOBA, *m/e* (2056.6), 2057.7 ($M^+ + 1$) (100), 1978.2 (70); ^1H NMR, (360 MHz, $CDCl_3$) δ, –0.46 (s, 6H, $(CH_3)_2SO$), 0.91 (t, 24H, $J = 7.2$ Hz, CH_3), 1.34 (m, 48H, $(CH_2)_3CH_3$), 1.97 (br s, 16H, OCH_2CH_2), 2.16 (m, 16H, $ArCHCH_2$), 3.88 (br s, 16H, OCH_2CH_2), 4.16 (d, 8H, $J = 7.2$ Hz, inner OCH_2O), 4.68 (t, 8H, $J = 7.2$ Hz, methine), 5.78 (d, 8H, $J = 7.2$, outer OCH_2O), 6.78 (s, 8H, Ar*H*). Anal. Calcd for $C_{122}H_{158}O_{25}S$ (2056.6): C, 71.25; H, 7.74; S, 1.56. Found: C, 71.02; H, 7.72; S, 1.42.

1·*p*-$I_2C_6H_4$. Into a Pyrex test tube capped with a rubber septum were placed 30.8 mg (0.014 mmol) of "empty **1**", 0.45 g (1.4 mmol) of *p*-$I_2C_6H_4$, and 5 mL of Ph_2O. This mixture was heated at 160 °C for 4.5 days. The mixture was cooled to 25 °C and poured into 50 mL of MeOH, and the precipitate that separated was filtered and chromatographed on silica gel with 2.5% EtOAc (v) in CH_2Cl_2 (see Tables I–III for yield, analytical, FABMS, and ^1H NMR data). This is procedure C.

1·$C_6H_5NH_2$. Into a Pyrex test tube capped with a rubber septum were placed 38.9 mg (0.017 mmol) of "empty **1**" and 5 mL of degassed 99.5+% aniline (Aldrich). This mixture was heated to 145 °C for 4.5 days. The product was isolated as in procedure C, and Tables I–III report yields, analytical, FABMS, and ^1H NMR data. This is procedure D.

Applications of procedure C or D to the other guests gave the other complexes, and Tables I–III report the yield, analytical, FABMS, and ^1H NMR results.

Decomplexation Rate Constants for 1·$(CH_3)_2NCOCH_3$. These rates were followed in degassed $C_6D_5NO_2$ by ^1H NMR spectral changes of incarcerated and free guest and concurrent changes in host by the same procedure reported for decomplexation of **3**·$(CH_3)_2NCOCH_3$ in $(CD_3)_2C_6D_4$.[3] Control experiments established that under the conditions of the experiment (time and temperature) essentially no **1**·$C_6D_5NO_2$ was formed.

Crystal Structure of 1·*p*-$I_2C_6H_4$·2$C_6H_5NO_2$. This complex crystallizes from $CHCl_3$–$C_6H_5NO_2$ as colorless parallelepipeds in the monoclinic system $P2_1/c$. Unit cell dimensions are as follows: $a = 16.777(2)$ Å, $b = 19.795(2)$ Å, $c = 20.327(2)$ Å, $\beta = 98.199(4)°$, $V = 6682$ Å^3, $Z = 2$. The crystal was examined on a modified Picker FACS-1 diffractometer, Mo Kα radiation, at –117 °C. The structure was determined by heavy atom methods. Refinement of 257 + 46 parameters (2 blocks, 2154 reflections with $I > 2\sigma(I)$, 7170 unique reflections) has an agreement value, *R*, currently at 0.11.

This hemicarceplex is centrosymmetric, and the two iodine atoms of the *p*-$I_2C_6H_4$ guest are located beyond the cavity area defined by the four $O(CH_2)_4O$ bridges. The crystal contains two nitrobenzene molecules per host, located in the region of the $CH_2CH_2C_6H_5$ groups.

Crystal Structure of 1·$O_2NC_6H_5$·2$C_6H_5NO_2$. This complex crystallizes from $C_6H_5NO_2$ as colorless parallelepipeds in the monoclinic system $P2_1/c$. Unit cell dimensions are as follows: $a = 16.757(1)$ Å, $b = 20.551(2)$ Å, $c = 20.106(2)$ Å, $\beta = 99.318(3)°$, $V = 6833$ Å^3, $Z = 2$. The crystal was examined on a modified Syntex $P\bar{1}$ diffractometer, Cu Kα radiation, at 298 K. The structure was determined by direct methods. Refinement of 260 + 46 parameters (2 blocks, 1876 reflections with $I > 2\sigma(I)$, 7588 unique reflections) has an agreement value, *R*, currently at 0.152. The centrosymmetric host contains one molecule of nitrobenzene at half-occupancy in positions related by the center of symmetry. The crystal contains two additional nitrobenzene molecules per host, located in the region of the $CH_2CH_2C_6H_5$ groups.

Crystal Structure of 1·*o*-BrC_6H_4OH·2$C_6H_5NO_2$. This complex crystallizes from $C_6H_5NO_2$ as small colorless parallelepipeds in the monoclinic $P2_1/c$. Unit cell dimensions are as follows: $a = 16.730(2)$ Å, $b = 20.493(2)$ Å, $c = 20.112(2)$ Å, $\beta = 99.779(4)°$, $V = 6795$ Å^3, $Z = 2$ (the host molecule is centrosymmetric). The *o*-BrC_6H_4OH guest is disordered in four positions in the host cavity with equal occupancy in all positions (two independent locations, each with an equivalent position related by the center of symmetry of the host). The bromine atom is in a position above or below the cavity region defined by the four $O(CH_2)_4O$ bridges. The crystal contains two nitrobenzene molecules per host, located in the region of the $CH_2CH_2C_6H_5$ groups. The crystal was examined on a modified Syntex $P\bar{1}$ diffractometer, Cu Kα radiation, at 298 K. The structure was determined by direct methods. Refinement of 257 + 62 parameters (2 blocks, 1330 reflections with $I > 2\sigma(I)$, 6221 unique reflections) has an agreement value, *R*, currently at 0.213.

Crystal Structure of 1·6H_2O·4*o*-$(CH_3)_2C_6H_4$. This complex crystallizes from *o*-xylene as colorless parallelepipeds in the triclinic system *P*1. Unit cell dimensions are as follows: $a = 16.728(3)$ Å, $b = 19.372(3)$ Å, $c = 25.468(4)$ Å, $\alpha = 71.631(3)°$, $\beta = 86.729(4)°$, $\gamma = 70.706(4)°$, $V = 7383$ Å^3, $Z = 2$. The crystal was examined on a modified Syntex $P\bar{1}$ diffractometer, Cu Kα radiation, at 298 K. The structure was determined by direct methods. Refinement of 483 + 111 parameters (2 blocks, 5873 reflections with $I > 2\sigma(I)$, 13518 unique reflections) has an agreement value, *R*, currently at 0.15.

This host seems to contain six water molecules (no hydrogen atoms have been located) in which the oxygen atoms occupy a roughly octahedral array with atoms about 2.8 Å apart. Although, for each of the three complexes described above, the two cavitand moieties are "eclipsed"; for this host a "Newman projection" down the centers of midpoints of the four oxygen atoms at the termini of the $O(CH_2)_4O$ bridges gives dihedral angles averaging 14.6°. This twist helps to bring the two planes containing these groups of four oxygen atoms 1 Å closer together than for the *p*-$I_2C_6H_4$ complex. The crystal contains four somewhat disordered *o*-xylene molecules per host, located in the region of the $CH_2CH_2C_6H_5$ groups and between the hosts.

Crystal Structure of 1·*p*-$(CH_3)_2C_6H_4$·2$C_6H_5NO_2$. This complex crystallizes from $CHCl_3$–$C_6H_5NO_2$ as small colorless rods in the monoclinic system $P2_1/c$. Unit cell dimensions are as follows: $a = 16.766(2)$ Å, $b = 20.442(3)$ Å, $c = 20.209(3)$ Å, $\beta = 99.183(5)°$, $V = 6837$ Å^3, $Z = 2$. The crystal was examined on a modified Syntex $P\bar{1}$ diffractometer, Cu Kα radiation, at 298 K. The structure was determined using the position parameters for the host of the *p*-$I_2C_6H_4$ complex. Refinement of the 249 + 49 parameters (2 blocks, 1490 reflections with $I > 2\sigma(I)$, 6251 unique reflections) has an agreement value, *R*, currently at 0.219. The centrosymmetric host contains one molecule of *p*-xylene disordered in two centrosymmetric positions of approximately equal occupancy. The two methyl carbons of each of the two possible positions overlap, as do the two para carbon atoms. The benzene rings are roughly perpendicular to each other and are aligned with each of the diagonals formed by the four bridge termini oxygen atoms. The crystal contains two nitrobenzene molecules per host, located in the region of the $CH_2CH_2C_6H_5$ groups.

Crystal Structure of 1·$(CH_3)_2NCOCH_3$·2$C_6H_5NO_2$. This complex crystallizes from $CHCl_3$–$C_6H_5NO_2$ in small colorless rods in the monoclinic system $P2_1/c$. Unit cell dimensions are as follows: $a = 16.740(2)$ Å, $b = 20.618(3)$ Å, $c = 20.033(3)$ Å, $\beta = 100.483(5)°$, $V = 6799$ Å^3, $Z = 2$. The crystal was examined on a modified Syntex $P\bar{1}$ diffractometer, Cu Kα radiation, at 298 K. The structure was determined by using the position parameters of the host from the complex containing $C_6H_5NO_2$. Refinement of 19 + 241 + 25 parameters (3 blocks, 1313 reflections with $I > 2\sigma(I)$, 5496 unique reflections) has an agreement value, *R*, currently at 0.223. The centrosymmetric host contains one molecule of $(CH_3)_2NCOCH_3$ disordered over several positions. The crystal contains two nitrobenzene molecules per host, located in the region of the $CH_2CH_2C_6H_5$ groups.

Details of the six crystal structures will be published elsewhere.